

## **Metabolic mitochondrial alterations prevail in the female rat heart 8 weeks after exercise cessation**

Carolina Tocantins <sup>1,2</sup>, João D. Martins <sup>1</sup>, Óscar M. Rodrigues <sup>1</sup>, Luís F. Grilo <sup>1,2</sup>, Mariana S. Diniz <sup>1,2</sup>, Jelena Stevanovic-Silva <sup>3</sup>, Jorge Beleza <sup>3</sup>, Pedro Coxito <sup>3</sup>, David Rizo-Roca <sup>3,4</sup>, Estela Santos-Alves <sup>3</sup>, Manoel Rios <sup>3</sup>, Lina Carvalho <sup>5</sup>, António J. Moreno <sup>1,6</sup>, António Ascensão <sup>3</sup>, José Magalhães <sup>3</sup>, Paulo J. Oliveira <sup>1</sup>, Susana P. Pereira <sup>1,3,\*</sup>

**Running title:** Exercise cessation heart mitochondria impact

Carolina Tocantins, MSc

1 - CNC – Center for Neuroscience and Cell Biology, CIBB – Centre for Innovative

Biomedicine and Biotechnology, University of Coimbra, 3004-531 Coimbra, Portugal

2 - PhD Programme in Experimental Biology and Biomedicine (PDBEB), Institute for

Interdisciplinary Research (IIIUC), University of Coimbra, 3004-531 Coimbra, Portugal

[ctsantos@cnc.uc.pt](mailto:ctsantos@cnc.uc.pt)

ORCID: 0000-0002-3758-0454

João D. Martins, MSc

1 - CNC – Center for Neuroscience and Cell Biology, CIBB – Centre for Innovative

Biomedicine and Biotechnology, University of Coimbra, 3004-531 Coimbra, Portugal

[jdgmartins@gmail.com](mailto:jdgmartins@gmail.com)

ORCID: 0000-0003-3676-3053

Óscar M. Rodrigues, MSc

1 - CNC – Center for Neuroscience and Cell Biology, CIBB – Centre for Innovative

Biomedicine and Biotechnology, University of Coimbra, 3004-531 Coimbra, Portugal

ORCID: 0000-0001-9714-2424

[osemmero@gmail.com](mailto:osemmero@gmail.com)

Luís F. Grilo, MSc

1 - CNC – Center for Neuroscience and Cell Biology, CIBB – Centre for Innovative

Biomedicine and Biotechnology, University of Coimbra, 3004-531 Coimbra, Portugal

2 - PhD Programme in Experimental Biology and Biomedicine (PDBEB), Institute for

Interdisciplinary Research (IIIUC), University of Coimbra, 3004-531 Coimbra, Portugal

[luís.grilo@uc.pt](mailto:luís.grilo@uc.pt)

ORCID: 0000-0002-6278-9241

Mariana S. Diniz, MSc

1 - CNC – Center for Neuroscience and Cell Biology, CIBB – Centre for Innovative

Biomedicine and Biotechnology, University of Coimbra, 3004-531 Coimbra, Portugal

2 - PhD Programme in Experimental Biology and Biomedicine (PDBEB), Institute for

Interdisciplinary Research (IIIUC), University of Coimbra, 3004-531 Coimbra, Portugal

[marianasdiniz.diniz@gmail.com](mailto:marianasdiniz.diniz@gmail.com)

ORCID: 0000-0002-2161-9676

Jelena Stevanovic-Silva, PhD

3 - Laboratory of Metabolism and Exercise (LaMetEx), Research Centre in Physical

Activity, Health and Leisure (CIAFEL), Laboratory for Integrative and Translational

Research in Population Health (ITR), Faculty of Sports, University of Porto, 4200-450

Porto, Portugal

[jela.stevanov@gmail.com](mailto:jela.stevanov@gmail.com)  
ORCID: 0000-0003-4641-1078

Jorge Beleza, PhD  
3 - Laboratory of Metabolism and Exercise (LaMetEx), Research Centre in Physical Activity, Health and Leisure (CIAFEL), Laboratory for Integrative and Translational Research in Population Health (ITR), Faculty of Sports, University of Porto, 4200-450 Porto, Portugal  
[jmsbeleza@gmail.com](mailto:jmsbeleza@gmail.com)  
ORCID: 0000-0002-7573-3757

Pedro Coxito, MSc  
3 - Laboratory of Metabolism and Exercise (LaMetEx), Research Centre in Physical Activity, Health and Leisure (CIAFEL), Laboratory for Integrative and Translational Research in Population Health (ITR), Faculty of Sports, University of Porto, 4200-450 Porto, Portugal  
[pedrocoxito@sapo.pt](mailto:pedrocoxito@sapo.pt)  
ORCID: 0000-0003-0573-7418

David Rizo-Roca, PhD  
3 - Laboratory of Metabolism and Exercise (LaMetEx), Research Centre in Physical Activity, Health and Leisure (CIAFEL), Laboratory for Integrative and Translational Research in Population Health (ITR), Faculty of Sports, University of Porto, 4200-450 Porto, Portugal  
4 - Department of Cell Biology, Physiology & Immunology, Faculty of Biology, University of Barcelona, Barcelona, Spain  
[rizeroca@gmail.com](mailto:rizeroca@gmail.com)  
ORCID: 0000-0002-9379-7543

Estela Santos-Alves, PhD  
3 - Laboratory of Metabolism and Exercise (LaMetEx), Research Centre in Physical Activity, Health and Leisure (CIAFEL), Laboratory for Integrative and Translational Research in Population Health (ITR), Faculty of Sports, University of Porto, 4200-450 Porto, Portugal  
[estelalves@gmail.com](mailto:estelalves@gmail.com)  
ORCID: 0000-0001-8084-0859

Manoel Rios, MSc  
3 - Laboratory of Metabolism and Exercise (LaMetEx), Research Centre in Physical Activity, Health and Leisure (CIAFEL), Laboratory for Integrative and Translational Research in Population Health (ITR), Faculty of Sports, University of Porto, 4200-450 Porto, Portugal  
[manoel.rios@hotmail.com](mailto:manoel.rios@hotmail.com)  
ORCID: 0000-0002-3574-6692

Lina Carvalho, MD PhD  
5 - Institute of Anatomical and Molecular Pathology, Faculty of Medicine, University of Coimbra, 3000-370 Coimbra, Portugal  
[lcarmo@chuc.min-saude.pt](mailto:lcarmo@chuc.min-saude.pt)  
ORCID: 0000-0001-8349-4488

António J. Moreno, PhD  
6 - Department of Life Sciences, School of Sciences and Technology, University of  
Coimbra, 3004-517 Coimbra, Portugal  
[matosmoreno@gmail.com](mailto:matosmoreno@gmail.com)  
ORCID: 0000-0003-3575-7604

António Ascensão, PhD  
3 - Laboratory of Metabolism and Exercise (LaMetEx), Research Centre in Physical  
Activity, Health and Leisure (CIAFEL), Laboratory for Integrative and Translational  
Research in Population Health (ITR), Faculty of Sports, University of Porto, 4200-450  
Porto, Portugal  
[aascensao@fade.up.pt](mailto:aascensao@fade.up.pt)  
ORCID: 0000-0001-5269-0857

José Magalhães, PhD  
3 - Laboratory of Metabolism and Exercise (LaMetEx), Research Centre in Physical  
Activity, Health and Leisure (CIAFEL), Laboratory for Integrative and Translational  
Research in Population Health (ITR), Faculty of Sports, University of Porto, 4200-450  
Porto, Portugal  
[jmaga@fade.up.pt](mailto:jmaga@fade.up.pt)  
ORCID: 0000-0003-4808-8374

Paulo J. Oliveira, PhD  
1 - CNC – Center for Neuroscience and Cell Biology, CIBB – Centre for Innovative  
Biomedicine and Biotechnology, University of Coimbra, 3004-531 Coimbra, Portugal  
[pauloliv@cnc.uc.pt](mailto:pauloliv@cnc.uc.pt)  
ORCID: 0000-0002-5201-9948

Susana P. Pereira, PhD  
1 - CNC – Center for Neuroscience and Cell Biology, CIBB – Centre for Innovative  
Biomedicine and Biotechnology, University of Coimbra, 3004-531 Coimbra, Portugal  
3 - Laboratory of Metabolism and Exercise (LaMetEx), Research Centre in Physical  
Activity, Health and Leisure (CIAFEL), Laboratory for Integrative and Translational  
Research in Population Health (ITR), Faculty of Sports, University of Porto, 4200-450  
Porto, Portugal  
[pereirasusan@gmail.com](mailto:pereirasusan@gmail.com)  
ORCID: 0000-0002-1168-2444

**\*Corresponding author**

Susana P. Pereira, PhD  
CNC - Center for Neuroscience and Cell Biology, UC Biotech, Biocant Park,  
University  
of Coimbra, 3060-197 Cantanhede, PORTUGAL,  
phone: +351-231-249-170,  
fax: 351-239-853409,  
email: [pereirasusan@gmail.com](mailto:pereirasusan@gmail.com)  
ORCID: 0000-0002-1168-2444

## **Acknowledgments**

This research was funded by the ERDF funds through the Operational Programme for Competitiveness–COMPETE 2020 and national funds by Foundation for Science and Technology under FCT-Post-doctoral Fellowship (SPP, SFRH/BPD/116061/2016), FCT-doctoral Fellowship (MSD, SFRH/BD/11934/2022; CT, SFRH/BD/11924/2022; LFG, SFRH/BD/5539/2020), project grant HORIZON-HLTH-2022-STAYHLTH-101080329-2; PTDC/DTP-DES/1082/2014 (POCI-01-0145-FEDER-016657), CENTRO-01-0246-FEDER- 000010 (Multidisciplinary Institute of Ageing in Coimbra), strategic projects UIDB/04539/2020, UIDP/04539/2020, LA/P/0058/2020, and EU's Horizon 2020 Research and Innovation program under the Marie Skłodowska-Curie Actions (No.722619, FOIE GRAS; No.734719, mtFOIE GRAS). It was also funded by the European Union (HORIZON-HLTH-2022-STAYHLTH-101080329). Views and opinions expressed are however these of the author(s) only and do not necessary reflect those of the European Union or the Health and Digital Executive Agency. Neither the European Union nor the granting authority can be held responsible for them. The funding agencies had no role in study design, data collection and analysis, decision to publish, or preparation of this document. There are no conflicts of interest associated with this work.

**Word count:** 9010 words

## **Abstract**

The consumption of high-caloric diets strongly contributes to the development of non-communicable diseases, including cardiovascular disease, the leading cause of mortality worldwide. Exercise (along with diet intervention) is one of the primary non-pharmacological approaches to promote a healthier lifestyle and counteract the rampant prevalence of non-communicable diseases. The present study evaluated the effects of exercise cessation after a short-period training on the cardiac metabolic and mitochondrial function of female rats. Seven-week-old female Sprague-Dawley rats were fed a control or a high-fat, high-sugar (HFHS) diet and, after 7 weeks, the animals were kept on a sedentary lifestyle or submitted to endurance exercise for 3 weeks (6 days per week, 20-60 min/day). The cardiac samples were analyzed 8 weeks after exercise cessation. The consumption of the HFHS diet triggered impaired glucose tolerance, whereas the HFHS diet and physical exercise resulted in different responses in plasma adiponectin and leptin levels. Cardiac mitochondrial respiration efficiency was decreased by the HFHS diet consumption, which led to reduced ATP and increased NAD(P)H mitochondrial levels, which remained prevented by exercise 8 weeks after cessation. Exercise training-induced cardiac adaptations in redox balance, namely increased relative expression of Nrf2 and downstream antioxidant enzymes persist after an eight-week exercise cessation period. In summary, endurance exercise modulated cardiac redox balance and mitochondrial efficiency in female rats fed a high-fat, high-sugar diet. These findings suggest that exercise may elicit cardiac adaptations crucial for its role as a non-pharmacological intervention for individuals at risk of developing non-communicable diseases.

**Keywords:** High-fat high-sugar diet; Female; Metabolic dysfunction; Mitochondria; Cardiac remodeling; Exercise cessation

## Background

Cardiovascular disease (CVD) is the leading cause of death worldwide. In 2020, CVD contributed to 19.1 million deaths globally<sup>1</sup>. Historically recognized as a disease of men, given the observed cardioprotective role of estrogen produced by women until menopause<sup>2</sup>, CVD is the principal cause of death in women, accounting for 35% of women's deaths worldwide in 2019<sup>3</sup>. Indeed, female-specific risk factors have been identified<sup>2</sup>. Besides common risk factors in both sexes, a faster increase in blood pressure elevation as well as a higher risk of cardiovascular events due to early-onset diabetes were observed in women at young ages (< 40 years) compared to men<sup>3</sup>. These occurrences are driven by insufficient CVD awareness among women and implication of the female sex in CVD-related clinical trials, letting CVD in women understudied, with dismissing diagnosis and intervention<sup>2-5</sup>. Other CVD risk factors include metabolic-related conditions, such as dyslipidemia, obesity, and diabetes, which strongly relate to unhealthy lifestyle habits, including an imbalanced diet and lack of physical activity.

The consumption of high-caloric diets has been a concern for a long time. Diets rich in saturated fats and added sugars, mainly based on industrialized and processed foods, have now become part of modern society<sup>6</sup>. The well-known Western diet is currently one of the paramount drivers of non-communicable diseases (NCDs) as it contributes to a variety of NCDs risk factors (i.e., increased visceral adiposity, hyperinsulinemia, elevated glycemia, hyperleptinemia, increased low-density lipoprotein (LDL) and triglycerides levels and decreased high-density lipoprotein (HDL)<sup>7,8</sup>, impacting the heart and cardiomyocytes<sup>9</sup>, and predisposing to type-2 diabetes and CVD incidence. Accordingly, a follow-up study analyzing the consumption of additional servings of ultra-processed food, revealed a 9% increased risk of CVD mortality among 3,003 adults<sup>10</sup>. One foremost goal of the United Nations (UN) is to reduce the number of premature deaths due to NCDs by 2030 through prevention and treatment, as stated in the 2030 Agenda for Sustainable Development.

Exercise is one of the non-pharmacological strategies used to reach the UN goal, given its association with a general improvement in metabolic health. Studies have shown that exercise contributes to the improvement of body composition, circulating biomarkers usually used as predictors of blood pressure and cardiometabolic risk<sup>11</sup>. Exercise is also associated with better cardiorespiratory fitness, decreased fasting insulin levels, higher insulin sensitivity, improved glucose homeostasis, and enhanced peripheral tissue oxygenation<sup>12-14</sup>. Despite this evidence, the type of exercise to be applied to a specific population, considering health conditions, age, sex, and lifestyle habits, is often questioned, and efforts are still being gathered for the guided implementation of lifestyle habits to counteract the NCDs rampant<sup>15,16</sup>. Moreover, low adherence or cessation of exercise training in the general population is a current concern<sup>17</sup>.

Cessation of physical exercise programs results in detraining. Detraining is the term used to describe the loss of the adaptations previously induced by training due to insufficient or in the absence of training stimulus<sup>18</sup>. The effects of detraining have been studied in the scope of CVD and aging<sup>18,19</sup> and may depend on factors, such as age, previous training level, duration of the cessation, and possibly other unexplored aspects. Within cardiomyocytes, the cardiac remodeling induced by exercise is reversed or abolished after a detraining period in hypertensive rats<sup>20</sup> and in mice with compromised insulin growth factor 1 (IGF-1) signaling<sup>21</sup>. But to date, cardiomyocyte-specific responses to detraining are widely undetermined.

The detraining period has been also associated with an increase in oxidative stress markers. Oxidative stress and mitochondrial dysfunction are highly implicated in the development of CVD<sup>22</sup>. Meanwhile, exercise has been shown to play a preventive or reversive role in developing mitochondrial dysfunction in the heart of mice with diabetic cardiomyopathy<sup>23</sup>. Mitochondria

isolated from the hearts of rats submitted to an exercise protocol exhibit a particular phenotype with increased levels of proteins involved in the antioxidant response<sup>24</sup> and Nuclear factor erythroid 2-related factor (Nrf2) signaling which are involved in the regulation of cellular redox balance in the heart as an adaptative response to exercise<sup>25</sup>. However, the implications of detraining on redox balance and mitochondrial efficiency and function are yet to be disclosed and understood<sup>18</sup>.

Previous studies have shown that understanding the detraining effects on cardiac remodeling regression might be as crucial as assessing the beneficial effects induced by physical exercise. Aside from the impact of the type and the duration of the training and exercise cessation periods, the implication of dietary habits on these effects is still understudied. The present study determined the effects of short-period exercise endurance training and consequent exercise cessation combined with a high-fat, high-sugar diet or control diet on females' cardiac metabolic and mitochondrial responses.

We hypothesized that a high-fat, high-sugar diet induces an adverse metabolic phenotype in the cardiac tissue impacting cardiac mitochondrial function and that a short-period exercise program (3 weeks) induces overall cardiac adaptations that remain detectable after cessation of physical exercise for 8 weeks.

## Materials and Methods

**Animals.** Seven-week-old female Sprague-Dawley rats (150-200 g) (Charles River, L'Arbresle, France) were fed a control (C) or high-fat, high-sugar (HFHS) diet. HFHS females were further divided into 2 subgroups: sedentary (S) and submitted to an endurance exercise protocol (E) which started at 14 weeks of age. Therefore, 3 experimental groups were considered in the present work: C-S – control diet and sedentary (n = 7); HFHS-S – HFHS diet and sedentary (n = 11); and HFHS-E – HFHS diet and exercised (n = 6) (Figure 1 A). The animals received food and water *ad libitum* and were housed in polyethylene type III-H cages with normal setting (21-22°C; 50-60% humidity, 12 h light/dark cycles), in a pathogen free animal facility at the Institute for Research and Innovation in Health – i3S (Porto, Portugal). The exercised animals (HFHS-E) were housed in polyethylene type IV cages equipped with a free-running wheel (Type 304 Stainless steel, Techniplast, Casale Litta, Italy) during the exercise protocol. In contrast, sedentary animals (C-S and HFHS-S) were not provided access to the running wheel. To promote the typical species behavior and psychological wellbeing, the cages were filled with corn cob bedding and enriched with shelter and nesting materials. During the experiment, the distribution of the different groups was blindly performed through allocation concealment by independent technicians. The experimental protocol was approved by the Ethical Committee of the Institute for Research and Innovation in Health – i3S, University of Porto, and National Government Authority (Direção Geral de Alimentação e Veterinária – No.0421/000/000/2018), in accordance with the Guidelines for Care and Use of Laboratory Animals in Research recommended by the Federation of European Laboratory Animal Science Associations (FELASA).

**Diets and exercise protocols.** The females consumed C or HFHS-diet (E157452-047 or D12451 (II) mod., Ssniff, Soest, Germany, respectively) starting at 7 weeks of age and throughout the 18 weeks of the experiment. The diet composition is presented in detail in Figure S1 A. At 14 weeks of age, the exercised females performed the endurance protocol on a motor-driven treadmill (LE8700, Panlab Harvard Apparatus, MA, USA) for 3 weeks, 6 days per week, and 20-60 min per day<sup>26</sup>. The females were adapted to the treadmill one week before initiating exercise protocols. The first week consisted of a gradual increasing activity ranging from 20 minutes to 60

minutes per day and from a minimum speed of 10 cm/s to a maximum speed of 30 cm/s. In the second and third weeks, the exercise protocol consisted of 60 minutes of activity with a program of increasing speed up to 35 cm/s. Through the entire period of exercise protocol, the females were housed in cages equipped with free-running-wheels to stimulate voluntary physical activity. The animals were weighed weekly, and all manipulations were performed during the active period of the animals (dark phase). The detailed description of the exercise protocol is provided in Figure S1 B.

**Glucose homeostasis.** An oral glucose tolerance test (OGTT) was performed before starting the exercise protocols (13 weeks old) and after a 6-hour fasting period. A dose of 2 g of glucose per kg body weight was orally administered in the form of the non-flavored jelly (Globo Gelatina Neutra, A Colmeia do Minho, Portugal)<sup>27</sup> avoiding a potential harm caused by intraperitoneal injection or oral gavage to the animals during the OGTT. The rats were previously trained to eat jelly without glucose. During the test, blood was removed from the tail vein at 15, 30, 60, 90 and 120 minutes after glucose administration. Blood glucose levels were also assessed at euthanasia using the tail prick test.

**Animal euthanasia and tissue sampling.** At 25 weeks of age the animals were anesthetized (induction: 5% isoflurane, 1 L/m O<sub>2</sub>; maintenance: 2.5% isoflurane, 0.4 L/m O<sub>2</sub>) between 8:00 and 10:00 am after overnight fasting. The abdominal cavity was exposed, and the blood was collected from the inferior vena cava and centrifuged (3000 g, 10 min, 4°C). Collected plasma was stored at -80°C. The heart was promptly collected, washed with ice-cold PBS, weighed, and the tissue was divided for mitochondria isolation and other analysis. The animals were labelled with a blindly assigned code to avoid bias.

**Isolation of heart mitochondria.** A segment of the heart was immersed in cold Heart Isolation Buffer (250 mM sucrose, 0.5 mM EGTA, 10 mM HEPES, pH 7.4 with KOH), supplemented with 0.1% fatty acid free bovine serum albumin (BSA) (A4503, Sigma; Saint Louis, USA) and finely minced. Cardiac mitochondria were isolated by a conventional differential centrifugation method with isolation medium supplemented with protease (Subtilisin A Type VIII 0.2 mg/g of tissue used, Sigma Aldrich, Madrid)<sup>28</sup>. Mitochondrial protein was determined by the biuret method<sup>29</sup>. An aliquot of the fresh mitochondrial fraction was used for in vitro oxygen consumption assays and mitochondrial membrane potential determination, while the remaining sample was stored at -80°C for later experiments.

**Mitochondrial oxygen consumption rates.** Mitochondrial respiratory function was measured using Biological Oxygen Monitor System and a Clark-Type oxygen electrode (Hansatech Instruments, England). Reactions were performed at 30°C in a magnetically-stirred glass chamber containing 1 mL of Heart Reaction Buffer (HRB - 130 mM sucrose, 10 mM HEPES, 65 mM KCl, 2.5 mM KH<sub>2</sub>PO<sub>4</sub>, 20 μM EGTA, pH 7.4) in which 0.5 mg cardiac mitochondria were suspended. Mitochondrial respiration stimulated via the electron transport chain (ETC) complex I or complex II was induced by adding glutamate/malate (G/M, 10 mM/5 mM) or succinate (10 mM) plus rotenone (1.5 μM, inhibitor of Complex I), respectively. State 3 and the phosphorylation cycle were obtained by adding ADP (200 nmol) and the oxygen consumption rate after ADP phosphorylation represented state 4. The state 3/state 4 ratio was used to obtain the respiratory control ratio (RCR). The ADP/O ratio represents the number of nmol of ADP phosphorylated per nmol O consumed during state 3. State 4 was measured in the presence of oligomycin (2 μg/ml) to inhibit proton influx through the ATP synthase.

**Mitochondrial membrane potential.** Mitochondrial membrane potential was indirectly assessed using a tetraphenylphosphonium (TPP<sup>+</sup>)-sensitive electrode. Mitochondrial membrane potential assays were performed using a mitochondrial suspension in HRB (0.5 mg/mL). For complex I assays, G/M (10 mM/5 mM) were used as substrate. Succinate (10 mM) was used as



the substrate for complex II assays, as well as rotenone 1.5  $\mu$ M. To induce a mitochondrial phosphorylative state ADP (200 nmol) was added to the chamber. A higher mitochondrial membrane potential leads to the accumulation of TPP<sup>+</sup>, allowing the establishment of the mitochondrial maximum membrane potential ( $\Delta\Psi$  max). The addition of ADP stimulates ATP production resulting in a depolarization in mitochondrial membrane potential.

**Quantification of hormones in plasma.** Adiponectin, leptin, IGF-1, and vaspin plasma circulating levels were quantified using specific ELISA kits manufactured by Mediatech GmbH (Germany, reference E09, E06, E25, and E106, respectively) according to manufacturer's instructions and using Synergy HT Microplate Reader (BioTek Instruments, Inc). The ideal dilution of the plasma was determined in a multi dilutions optimization step.

**Histological analysis.** Cardiac tissue was fixed in 4% paraformaldehyde (pH 7.4), dehydrated in a graded series of alcohol (70-100%) and embedded in paraffin. The paraffin blocks with the embedded cardiac tissue were carefully trimmed at 10  $\mu$ m using a LEICA RM2255 microtome obtaining the whole extension of the tissue samples. Paraffin sections were trimmed to a final thickness of 3  $\mu$ m for hematoxylin and eosin (H&E) staining and Masson's Trichrome staining. In each technique, the mounting of the histological slides was performed by Sakura Tissue-Tek GLS. The microscopic images were acquired in a Nikon ECLIPSE Ci microscope with a Nikon Ds-Fi 3 camera (Nikon Europe BV, Amsterdam, Netherlands). Analysis of the stained heart sections was performed by a proficient pathologist.

**Immunohistochemistry.** The immunohistochemical study was performed in the heart tissue using Bond Polymer Refine Detection™ (DS9800 Leica Biosystems, Newcastle, United Kingdom) on BondMax, according to the manufacturer's instructions. After performing the antigen retrieval, Peroxide Block was used and the primary antibody against Vimentin (ready-to-use, clone V9, PA0640, LEICA Biosystems) was applied to the sections.

**Protein quantification.** Protein concentration of the cardiac tissue lysates or cardiac mitochondrial fraction were determined using the Pierce™ BCA Protein Assay Kit or Pierce™ Protein Assay from Thermo Fisher Scientific (Illinois, USA), according to the manufacturer's instructions and using BSA dilutions as standards, prepared in the corresponding extraction buffer.

**Western blotting.** The cardiac tissue was homogenized three times during 20 seconds with an Ultra-Turrax homogenizer from IKA (Staufen, Germany) in RIPA buffer (50 mM Tris pH 8.0, 150 mM NaCl, 5 mM EDTA, 15 mM MgCl<sub>2</sub>, 1% Triton X-100) supplemented with 0.5 mM PMSF, 20 mM NaF, 10 mM NAM, 5 mM Sodium Butyrate, 100 mM Orthovanadate, 0.5% DOC, and 2.5% protease inhibitor cocktail (containing 104 mM AEBSF, 80  $\mu$ M Aprotinin, 4 mM Bestatin, 1.4 mM E-64, 2 mM Leupeptin and 1.5 mM Pepstatin). After supplementation with Laemmli buffer, the samples were boiled at 95°C for 5 min. Samples were loaded in 10% acrylamide gels and electrophoresis performed at 30 mA per gel. Protein was transferred to PVDF membranes in a Trans-Blot Cell (Bio-Rad, California, USA). The membranes were blocked in 5% BSA for 1 hour at room temperature, incubated with the primary antibody overnight (Table S1) and respective secondary antibody for 2 hours (Table S2). Clarity Western ECL Substrate (Bio-Rad, California, USA) was used to develop the membranes and the images were collected with a Gel Documentation System Imager (VWR, Pennsylvania, USA), analyzed with the TotalLab TL120 software (Nonlinear Dynamics, Newcastle, UK) and the results normalized by Ponceau staining (Ponceau S, Alfa Aesar, Massachusetts, USA) and to the C-S average, considered = 1.

**Real-Time PCR analysis.** For the quantitative assessment of mRNA expression, total RNA was extracted from 30 – 40 mg of cardiac tissue using TripleXtractor RNA extraction reagent (GRiSP Research Solutions, Porto, Portugal) and purified using the RNeasy® Mini Kit

(QIAGEN, Hilden, Germany), according to the manufacturer's instructions. The RNA concentration was quantified using a NanoDrop™ 2000 spectrophotometer (Thermo Fisher Scientific, Massachusetts, USA) and the RNA's integrity was assessed with Experion™ RNA StdSens (Bio-Rad, California, USA). Synthesis of cDNA was performed using iScript™ cDNA Synthesis Kit (Bio-Rad, California, USA). Real-time PCR was performed using the fluorescent dye SsoFast™ EvaGreen Supermix in a CFX96 Touch™ Real-Time PCR Detection System (Bio-Rad, California, USA) and the reaction was set with the software CFX Manager™ 3.1 (Bio-Rad, California, USA). The relative expression of target genes was normalized for 18S rRNA,  $\beta$ -actin and GAPDH housekeeping gene expression and to the C-S average, considered = 1. The list of primers is given in Table S3.

**Measurement of ATP and NAD(P)H level.** The ATP levels were assessed in the heart's mitochondrial fraction using the CellTiter-Glo Luminescent Cell Viability Assay (Promega, WI, USA). NAD(P)H levels were measured using NAD(P)H-Glo Detection System (Promega, WI, USA) according to the manufacturer's instructions. The detailed methodology description is provided in the Supplementary Material.

**Enzymatic activities.** Catalase activity was determined by following hydrogen peroxide decomposition as previously described<sup>30</sup>. Creatine kinase activity was determined by an adapted protocol of Creatine Kinase BR (Linear Chemicals, Barcelona, Spain). Glucose-6-phosphate dehydrogenase activity was determined by adapting the previously described protocol<sup>31</sup>. The enzyme activity of hexokinase was determined as previously described<sup>32,33</sup>. Lactate dehydrogenase activity was determined adapting the protocol previously described<sup>34</sup>. The detailed methodology description of each enzymatic activity is provided in the Supplementary Material.

**Data analysis and statistics.** Comparison between the experimental groups (C-S, HFHS-S and HFHS-E) was performed using one-way ANOVA or Kruskal-Wallis according to the normality of the groups (tested with the Shapiro-Wilk test, with  $\alpha = 0.05$ ) and, when significant ( $p < 0.10$ ), was followed by multiple comparisons through unpaired t-test or Mann-Whitney according to the normality of the groups. Outliers were discovered with the ROUT method, with  $Q = 2\%$ . Data were analyzed using GraphPad Prism 8.0.2 (GraphPad Software, Irvine, CA, USA) and results are represented as median, 1<sup>st</sup> quartile ( $Q_1$ ), and the 3<sup>rd</sup> quartile ( $Q_3$ ) with three significant digits and expressed as F-value (F), and degrees of freedom (DF). For the computational analysis, Orange version 3.26.0 was used. All data were preprocessed for further analysis, including imputing missing values with the average/most frequent values and normalization to the interval [-1,1]. The Principal Component Analysis (PCA) computes the PCA linear transformation of the input data transforming dataset with weights of individual instances or weights of principal components represented in a scatter plot. For the linear projection, all the combinations of the features were computed to identify the top-scoring parameters that better distinguish the two-dimensional data according to the experimental groups through the Mean Squared Error of the k-nearest neighbors classifier.

## Results

### *Model characterization and glucose homeostasis*

Generally, HFHS diet causes metabolic dysfunction with repercussions in physiology and molecular mechanisms<sup>35</sup>. Given the susceptibility to body weight gain and impaired glucose handling when fed with HFHS diet, the animals' body weight and their glucose metabolism capacity were determined during the experiment. No statically significant alterations were

detected in the body weight of the females throughout the experiment (Figure 1 B), despite the 5-8% body weight decrease of the exercised females during exercise protocols when compared to the HFHS-S group. Nevertheless, a normal body weight range is not in a direct association with healthy metabolism<sup>35,36</sup>. Considering this, the glucose metabolism was evaluated through OGTT before the beginning of the exercise protocol (Figure 1 C). Before starting the exercise protocol, the animals subjected to the HFHS diet already had impaired glucose tolerance (diet effect:  $p = 0.0049$ ), with a difference in basal glucose levels ( $p = 0.016$ ). The glucose area under the curve (AUC), as an index of whole glucose excursion after glucose loading (Figure 1 D) was higher in females fed with the HFHS diet (HFHS-S vs C-S: F-value (F) = 1.368, degrees of freedom (DF) = 15,  $p = 0.001$ ). No statically significant alterations were observed in the capillary glucose levels assessed at euthanasia (Figure 1 E).

The mass of the heart and brain were assessed in the different experimental groups. No alterations regarding heart mass (Figure 1 F), heart-to-body weight ratio (Figure S1 C), brain mass (Figure S1 D) or the heart-to-brain mass ratio (Figure S1 E) were observed.

#### *Assessment of hormonal imbalance and its impact on metabolic health in female rats subjected to a high-fat high-sugar diet with sedentary behavior and exercise intervention*

Hormonal imbalance can impact metabolic health, and the hormones typically secreted by adipose tissue and liver play a crucial role in regulating immune processes involved in chronic low-grade inflammation<sup>37</sup>. The levels of several hormones secreted by the adipose tissue and liver were assessed in the plasma of the female rats. The animals subjected to the HFHS diet and sedentary lifestyle showed increased levels of plasma adiponectin (Figure 2 A) compared to the control group (HFHS-S vs C-S: F = 2.462, DF = 8,  $p = 0.019$ ). This increase was reversed by exercise that led to decreased values compared to the HFHS-S group and values similar to the control group (Z = 2.601,  $p = 0.005$ ). The levels of leptin (Figure 2 B) were decreased in the plasma of females engaged in the exercise protocol compared with both control and HFHS-S groups (HFHS-E vs C-S: F = 5.830, DF = 5,  $p = 0.010$ ; HFHS-E vs HFHS-S: F = 4.232, DF = 7,  $p = 0.046$ ). The plasma levels of the adipokine vaspin of females subjected to the HFHS diet with a sedentary behavior were found to be 44% lower than the control group, despite not being statistically significant (Figure 2 C). The levels of IGF-1 (Figure 2 D), a hormone primarily produced by the liver, were decreased in the plasma of the female rats with a HFHS diet and a sedentary behavior compared to the control group (HFHS-S vs C-S: F = 1.727, DF = 7,  $p = 0.027$ ).

Additional parameters related to hepatic metabolism (aspartate transaminase (AST), alanine aminotransferase (ALT), and urea), muscle injury (creatine kinase (CK), creatinine), and cardiometabolic risk predictors (HDL, LDL, total cholesterol, triglycerides) have been previously reported<sup>26</sup> and were incorporated in a principal component analysis (PCA) for a better characterization of the experimental groups. Although no clear separation between the groups was observed when considering all plasma parameters (Figure S2 A), our results revealed that the hormones adiponectin and leptin emerged as key features with higher impact to separate the samples based on the experimental condition (C-S, HFHS-S, and HFHS-E) (Figure 2 E).

#### *Cardiac tissue morphological analysis and indicators of hypertrophy in response to an high-fat high-sugar diet and exercise intervention in female rats*

The histological analysis of the cardiac tissue allows the morphological characterization of the heart and the evaluation of indicators of possible hypertrophy. Loss of the integrity of the perivascular matrix surrounding the cardiac blood vessels is associated with atherosclerotic

processes, a common cardiovascular complication<sup>38</sup>. The morphological alterations in the cardiac tissue of the different experimental groups were evaluated by histological analysis (Figure 3). The cardiac H&E staining (Figure 3 A) revealed no differences in the heart morphology between the groups. The cardiac cells demonstrated similar shape and size. Although H&E allows the visualization of the perivascular matrix it does not stain collagen fibers, a main component of the perivascular matrix. The Masson's Trichrome staining (Figure 3 B) enables the detection of collagen fibers in the perivascular matrix surrounding the vessels of the cardiac tissue. A mild enlargement of the perivascular matrix is observed in the cardiac tissue of HFHS-S females, and of HFHS-E females, compared to C-S. Increased deposition of collagen fibers, perceived by the intense blue color surrounding the blood vessels of the myocardium, is observed in both HFHS groups. This is also corroborated by the observation of a stronger vimentin staining (Figure 3 C), marked by the darker brown color surrounding the vessels. Vimentin is an interfilamentous protein of the cardiac tissue, and its increased expression is commonly observed in association with cardiac fibrosis<sup>39</sup>.

Low-grade systemic inflammation is a common indicator of morbidity and is often associated with metabolic imbalance induced by the HFHS diet<sup>40,41</sup>. To evaluate the potential effects of the diet in the females hearts, we measured the levels of proteins that serve as markers of inflammation and cardiac damage (Figure 3 D and Figure S3). However, the protein levels of cardiac troponin T, interleukin 6 (IL-6), and tumor necrosis factor  $\alpha$  (TNF $\alpha$ ) did not reach statistically significant differences between the groups.

#### *Modulation of female cardiac metabolism plasticity by high-fat high-sugar diet and exercise*

Metabolic dysfunction might induce changes in insulin sensitivity, impairing insulin signaling and its downstream targets essential for cellular function and survival<sup>42</sup>. The levels of proteins involved in the insulin signaling pathway were evaluated. No differences were observed in the levels of the main protein responsible for glucose uptake in the heart, glucose transporter type 4 (GLUT4) (Figure S4 A), or insulin signaling cascade initiation, insulin receptor substrate 1 (IRS-1) (Figure S4 B). Protein kinase B (Akt) is a central kinase to many signalling pathways within the heart that ensure cardiac growth, homeostasis and survival<sup>43</sup>. Although the levels of total Akt (Figure S4 C) and phosphorylated Akt at the Ser 473 residue (Figure S4 D) were not significantly different between the experimental groups, the ratio of the phosphorylated Akt to total Akt (Figure 4 A) was tendentially increased in the hearts of females that were exercised compared to the control group (HFHS-E vs C-S: median = F = 16.81, DF = 5, p = 0.095). Conversely, the levels of Akt phosphorylated at the residue Thr 308 (Figure S4 E), which is important for optimal Akt activation, and its ratio to total protein (Figure S4 F), were similar between the groups. However, in the downstream signaling, the relative expression of the phosphorylated form of P70 (or S6K) (Figure 4 B) was increased in the hearts of exercised females compared to both control and HFHS-S groups (HFHS-E vs C-S: F = 2.195, DF = 5, p = 0.068; HFHS-E vs HFHS-S: F = 3.135, DF = 5, p = 0.016). Despite the observed differences in p-P70 levels, no alterations were observed in the ratio between its phosphorylated form (Figure S4 H) and total protein (Figure S4 G). A known downstream target of Akt is one of the proteins involved in the cellular anabolic program, glycogen synthase kinase 3 (GSK3)<sup>43</sup>. The two isoforms of GSK3 (GSK3  $\alpha$  and GSK3  $\beta$ ) were evaluated in the cardiac tissue of the female rats. Nevertheless, no alterations were observed in the levels of the total protein isoforms (Figure 4S I and L) their phosphorylated forms (Figure S4 J and M), or in the ratio between the phosphorylated and total forms for each isoform (Figure S4 K and N). The protein levels of AMP-activated protein kinase (AMPK) isoform  $\alpha$  were evaluated in the cardiac tissue. The protein AMPK is involved in

energy balance in the heart<sup>44</sup>. No alterations were observed in the levels of total AMPK $\alpha$  (Figure S4 O), or in the levels of the phosphorylated protein (activated) at the residue Thr 172 (Figure S4 P). Nonetheless, HFHS females showed increased levels of the ratio of the phosphorylated form of this protein in the residue Thr 172 to total AMPK $\alpha$  (Figure 4 C). This effect was less evident in the hearts of females with a sedentary lifestyle (HFHS-S vs C-S:  $F = 22.23$ ,  $DF = 6$ ,  $p = 0.099$ ), but exacerbated in the females subjected to exercise, compared to control females (HFHS-E vs C-S: median =  $F = 4.886$ ,  $DF = 5$ ,  $p = 0.003$ ).

Maintenance of the cardiac metabolic flexibility is essential for cardiac homeostasis and alterations in substrate utilization in the heart, atypical plasticity, may relate to cardiac dysfunction<sup>45</sup>. Hypoxia-inducible factor 1-alpha (HIF1 $\alpha$ ) can be induced in response to hyperglycemia<sup>46</sup>. The levels of the transcript *Hif1 $\alpha$*  (Figure 4 D) were increased in the hearts of female rats subjected to the HFHS diet and exercise compared to females fed only with the HFHS diet and kept sedentary (HFHS-E vs HFHS-S:  $F = 2.149$ ,  $DF = 5$ ,  $p = 0.036$ ). Cardiac alterations in the *Hif1 $\alpha$*  transcript levels were accompanied by variations in the levels of the transcripts of proteins involved in fatty acid metabolism. The transcript levels of the peroxisomal acyl-coenzyme A oxidase 1 (*Acox1*) (Figure 4 E), were tendentially increased in the hearts of exercised females compared to both control and the HFHS sedentary groups (HFHS-E vs C-S:  $F = 6.867$ ,  $DF = 4$ ,  $p = 0.062$ ; HFHS-E vs HFHS-S:  $F = 3.112$ ,  $DF = 4$ ,  $p = 0.068$ ). On the other hand, the levels of the transcripts from peroxisome proliferator-activated receptor alpha (*Ppara*) (Figure 4 F) were slightly decreased in the hearts of females that consumed the HFHS diet but were kept sedentary throughout the experiment, compared to the control group (HFHS-S vs C-S:  $F = 1.537$ ,  $DF = 10$ ,  $p = 0.076$ ). In the cardiac tissue of females subjected to exercise while fed the HFHS diet, *Ppara* transcript levels were lower compared to the females from the control and HFHS sedentary groups (HFHS-E vs C-S:  $F = 2.527$ ,  $DF = 3$ ,  $p = 0.002$ ; HFHS-E vs HFHS-S:  $F = 3.885$ ,  $DF = 10$ ,  $p = 0.041$ ). The maximum activity of enzymes involved in glucose metabolism pathways, such as hexokinase, glucose-6-phosphate dehydrogenase, and lactate dehydrogenase (Figure 4 G, H, and I, respectively), were similar in all experimental groups.

#### *The impact of high-fat high-sugar diet and exercise cessation on cardiac mitochondrial performance*

Increased levels of activated AMPK $\alpha$  might relate to increased AMP levels and alterations in ATP production. The heart is highly dependent on ATP production within mitochondria. Therefore, maintaining the balance of mitochondrial processes is vital for heart energetic demands and function. The mitochondrial oxygen consumption rates and membrane potential were evaluated in isolated cardiac mitochondria to understand the impact of the HFHS diet and exercise cessation 8 weeks after short period training while fed with the HFHS diet in the females' hearts. Complex I supported cardiac mitochondrial bioenergetics revealed that mitochondrial state 2 (Figure 5 A) was increased in the group that was subjected to exercise, compared to the control group (HFHS-E vs C-S:  $F = 1.401$ ,  $DF = 6$ ,  $p = 0.012$ ). Higher mitochondrial state 4 respiration rates values (Figure 5 C) contributed to the observed decreased respiratory control ratio (RCR, calculated as the ratio between mitochondrial states 3 and 4) (Figure 5 D), especially in the exercised group in which this parameter was significantly increased compared to the control group (HFHS-E vs C-S: median =  $F = 1.871$ ,  $DF = 6$ ,  $p = 0.022$ ), and since no alterations were observed in mitochondrial state 3 (Figure 5 B). The RCR (Figure 5 D) was decreased in the heart of females subjected to the HFHS diet independently of exercise when compared to the control group (HFHS-S vs C-S:  $F = 3.555$ ,  $DF = 6$ ,  $p = 0.011$ ; HFHS-E vs C-S:  $F = 3.335$ ,  $DF = 6$ ,  $p = 0.031$ ). A decrease in HFHS-S and HFHS-E cardiac mitochondria coupled efficiency supported by

complex-I (decreased ADP/O values) (Figure 5 E) was also observed, being more pronounced in females that had an HFHS diet and a sedentary behavior, compared to the control group (HFHS-S vs C-S:  $F = 26.40$ ,  $DF = 6$ ,  $p = 0.029$ ; HFHS-E vs C-S:  $F = 49.38$ ,  $DF = 6$ ,  $p = 0.085$ ). Regarding complex-II supported cardiac mitochondrial respiration supported with succinate, the mitochondrial state 2 (Figure 5 F) was increased in the cardiac mitochondria of females subjected to the HFHS diet and exercise compared to the control and HFHS-S groups (HFHS-E vs C-S:  $F = 2.196$ ,  $DF = 6$ ,  $p = 0.051$ ; HFHS-E vs HFHS-S:  $F = 1.417$ ,  $DF = 10$ ,  $p = 0.047$ ). No alterations were observed in mitochondrial respiration states 3 and 4 (Figure S5 A and B, respectively) resulting in unaltered RCR (Figure S5 C) and ADP/O (Figure S5 D) values.

During oxidative phosphorylation, protons are pumped across the inner mitochondrial membrane from the matrix to the intermembrane space, establishing a voltage difference across the membrane, known as the mitochondrial membrane potential ( $\Delta\Psi$ ), being proportional to the proton motive force, a critical factor in ATP synthesis and mitochondrial function. A similar development of maximum mitochondrial membrane potential ( $\Psi_{\max}$ ) using complex I substrates was observed between the experimental groups (Figure S5 E). Physical exercise combined with the HFHS diet predisposed rat cardiac mitochondria to higher mitochondrial membrane depolarization upon ADP administration ( $\Delta\Psi$  ADP, Figure 5G), compared to the control and HFHS-S group (HFHS-E vs C-S:  $F = 6.816$ ,  $DF = 5$ ,  $p = 0.033$ ; HFHS-E vs HFHS-S:  $F = 3.139$ ,  $DF = 5$ ,  $p = 0.077$ ). However, mitochondrial repolarization was similar between the groups (Figure S5 F) and no differences were observed in the time cardiac mitochondria took to completely phosphorylate the added ADP (ADP phosphorylation or lag phase) (Figure S5 G). Using complex II substrates, isolated cardiac mitochondria from both HFHS groups showed higher depolarization with ADP ( $\Delta\Psi$  ADP, Figure 5 I), compared with the control group (HFHS-S vs C-S:  $F = 6.729$ ,  $DF = 10$ ,  $p = 0.009$ ; HFHS-E vs C-S:  $F = 84.83$ ,  $DF = 5$ ,  $p = 0.022$ ).  $\Delta\Psi$  ADP was also significantly higher in HFHS fed exercised females than in sedentary ones (HFHS-E vs HFHS-S:  $F = 12.61$ ,  $DF = 5$ ,  $p = 0.049$ ) and cardiac mitochondria from exercised females also showed increased  $\Psi_{\max}$  (Figure 5 H), compared to the control group (HFHS-E vs C-S:  $F = 12.06$ ,  $DF = 6$ ,  $p = 0.012$ ). Nevertheless, cardiac mitochondria from all groups had similar repolarization (Figure S5 H) and exhibited similar rates of ADP phosphorylation, taking similar time to completely phosphorylate the added ADP (Figure S5 I).

#### *Cardiac mitochondrial markers variations in response to an high-fat high-sugar diet and exercise intervention*

To clarify the induced alterations in cardiac mitochondrial bioenergetics, the protein and transcript levels of several mitochondrial biomarkers were evaluated (Figure 6). The protein encoded by the RNA polymerase mitochondrial (*Polrmt*) gene is responsible for the transcription of mitochondrial DNA, being involved in mitochondrial DNA expression<sup>47</sup>. In the cardiac tissue, *Polrmt* transcript levels (Figure 6 A) were decreased in both groups of females subjected to the HFHS diet, independently of exercise (HFHS-S vs C-S:  $F = 7.536$ ,  $DF = 3$ ,  $p = 0.010$ ; HFHS-E vs C-S:  $F = 56.78$ ,  $DF = 3$ ,  $p = 0.045$ ). The protein levels of TOM20, a known mitochondrial mass indicator, were evaluated but no differences were observed (Figure 6 B). However, the evaluation of the protein levels of the mitochondrial complex III subunit UQCRC2 (Figure 6 C) showed a decreased relative expression in the hearts of HFHS-E females, compared to the control group (HFHS-E vs C-S:  $F = 1.629$ ,  $DF = 5$ ,  $p = 0.038$ ), and a tendentially decreased expression when compared with the HFHS-S group (HFHS-E vs HFHS-S:  $Z = 2.169$ ,  $p = 0.067$ ). The protein levels of other subunits from the different respiratory chain complexes (NDUFB8 – CI; SDHB – CII;

MTCO2 – CIV; ATP5A – ATP synthase) were unaltered by the experimental conditions (Figure S6 A).

Mitochondria endure constant fusion and fission processes, crucial to maintain their characteristics and function. Together with mitochondrial biogenesis and mitophagy, these processes enable the maintenance of mitochondrial quality<sup>48</sup>. The levels of proteins involved in mitochondrial biogenesis and dynamics were evaluated. No alterations were observed between the experimental groups for the evaluated proteins related with mitochondrial biogenesis mitochondrial transcription factor A (TFAM) (Figure S6 B) and peroxisome proliferator-activated receptor- $\gamma$  coactivator (PGC1 $\alpha$ ) (Figure S6 C). The levels of the proteins mitochondrial fission 1 protein (FIS1) (Figure S6 D) and dynamin-related protein 1 (DRP1) (Figure S6 E), involved in mitochondrial fission, were also unaltered, as well as the relative expression of OPA1 mitochondrial dynamin like GTPase (OPA1) (Figure S6 F), mitofusin 1 (MFN1) (Figure S6 G), and mitofusin 2 (MFN2) (Figure S6 H), proteins involved in mitochondrial fusion processes.

Changes in the levels of donor molecules (e.g., electrons, protons, phosphate donors) and molecules involved in energy balance may be implicated in mitochondrial bioenergetic alterations<sup>49</sup>. The levels of ATP and NAD(P)H were evaluated in the mitochondrial fraction of the female rats' hearts. A decrease in the levels of ATP (Figure 6 D) was observed in the cardiac mitochondria of females subjected to an HFHS diet and a sedentary lifestyle compared to the control group (HFHS-S vs C-S:  $F = 1.753$ ,  $DF = 6$ ,  $p = 0.039$ ) which was *ameliorated by physical exercise while on the HFHS diet*. On the other end, the levels of NAD(P)H (Figure 6 E) in the cardiac mitochondrial fraction of the HFHS-S group were significantly increased, compared to the control group (HFHS-S vs C-S:  $F = 3.613$ ,  $DF = 9$ ,  $p = 0.028$ ) and normalized with the exercise. Creatine Kinase (CK) plays a critical role in maintaining the energy balance in cells with high energy demands, such as cardiac muscle cells. CK catalyzes the transfer of a phosphate group from phosphocreatine to ADP to form ATP, providing a rapid source of ATP for energy-demanding processes and allowing the tight control of ADP and ATP concentrations in the heart. Nevertheless, the determined activity of CK (Figure 6 F) in the cardiac tissue of the female rats was similar between the different experimental groups.

#### *Exercise-induced upregulation of Nrf2 and antioxidant enzymes in high-fat high-sugar -fed female hearts*

*Mitochondrial homeostasis dysregulation and potential damage may contribute to an unbalanced compartmentalized redox state. Whenever ROS production increases, especially of the superoxide anion, the antioxidant defense systems takes action to prevent further damage and maintain homeostasis<sup>50</sup>. Nuclear factor erythroid 2-related factor plays a crucial role regulating antioxidant defenses enzymes' gene expression, consequently playing a critical role in redox balance<sup>51</sup>. Increased levels of Nrf2 (Figure 7 A) were detected in the hearts of HFHS-E females compared to both control and HFHS sedentary groups (HFHS-E vs C-S:  $F = 3.999$ ,  $DF = 4$ ,  $p = 0.021$ ; HFHS-E vs HFHS-S:  $F = 1.097$ ,  $DF = 8$ ,  $p = 0.032$ ). In the heart, Nrf2 directly regulates the levels of glutathione peroxidase 4 (GPX4), superoxide dismutase 1 (SOD1) and catalase proteins<sup>51</sup>. Accordingly, the levels of GPX4 (Figure 7 B) were increased in HFHS-E females compared to the control and HFHS-S group (HFHS-E vs C-S:  $F = 15.27$ ,  $DF = 4$ ,  $p = 0.008$ ; HFHS-E vs HFHS-S:  $Z = 2.594$ ,  $p = 0.019$ ). Although no statistically significant changes were detected in SOD1 protein levels in the cardiac tissue (Figure 7 C), a similar behavior was observed in the group of females that consumed the HFHS diet and were exercised. The cardiac enzymatic activity of catalase was also assessed being the more pronounced effect found in the hearts of exercised animals, despite the consumption of the HFHS diet. HFHS diet itself also led*

to increased catalase activity (Figure 7 D; HFHS-S vs C-S:  $F = 4.353$ ,  $DF = 10$ ,  $p = 0.042$ ; HFHS-E vs C-S:  $F = 1.095$ ,  $DF = 5$ ,  $p = 0.019$ ).

## Discussion

The consumption of diets high in fat and sugars is widespread in industrialized countries<sup>6</sup>, with a clear association with the rampant numbers of NCDs, where CVD is the number one cause of death globally. Consequently, studies have demonstrated that the consumption of the so-called Western diet results in the development of metabolic dysfunction and mitochondrial impairment<sup>6</sup>. Although regular physical exercise can have beneficial effects counteracting the cardiac alterations induced by obesity, diabetes, and other metabolic dysfunctions often related to unhealthy dietary habits, concerns remain regarding the potential implications of detraining on cardiac function<sup>17</sup>.

Animal models are essential to studying human diseases and elucidating the underlying mechanisms involved in the condition's pathophysiology. However, most of the existing knowledge was obtained from experiments performed solely on male animals, limiting the applicability of these findings to both sexes. Here, we investigated the metabolic and mitochondrial alterations occurring in the hearts of female rats subjected to a high-fat high-sugar diet and short-term exercise intervention followed by an eight-week period of exercise cessation, evidencing the alterations prevailing in the female rats' heart.

One of the most common outcomes of high-caloric diets and sedentary lifestyles is an increase in body weight. Overweight and obese individuals are more prone to metabolic syndrome and type 2 diabetes development due to low-grade systemic inflammation, insulin resistance, hyperglycemia, and other indicators of metabolic dysfunction<sup>52</sup>. In the current study, the female rats fed with the HFHS diet did not develop obesity during the experiment. There have been reports of metabolic dysfunction in the absence of obesity, and several terms have been used to describe the metabolically unhealthy normal weight phenotype<sup>35</sup>.

The evaluation of circulating hormones secreted by the adipose tissue is often used to detect metabolic dysfunction since adipokines are implicated in the inflammatory response and play a role in regulating other tissues' metabolism<sup>53</sup>. It is described that elevated circulating leptin levels and decreased adiponectin levels contribute to inflammation and cardiovascular dysfunction<sup>52</sup>. Interestingly, in our study, the females subjected to the HFHS diet that did not exercise showed increased levels of adiponectin. Despite the controversy, other studies have reported the same. High-sucrose diet-fed male Wistar rats showed increased adiponectin plasma levels until the 24<sup>th</sup> week of diet consumption decreasing at week 48 after metabolic syndrome establishment<sup>54</sup>. Another study showed that high-fat, high-glucose diet-fed male Wistar rats displayed increased adiponectin circulating levels regardless of the increased body weight after 20 weeks on the diet<sup>55</sup>. This may indicate that in this animal model, during the initial phase of metabolic dysfunction, circulating adiponectin levels increase as a response to the first stages of metabolic imbalance and may therefore be implicated in metabolic dysfunction progression. Indeed, in our study, exercise-related adaptations even after the cessation of training contributed to the prevention of this outcome, and exercised females fed with the HFHS diet showed similar adiponectin levels to those of the control group. On the other hand, the exercise intervention resulted in significantly decreased levels of circulating leptin even in relation to the HFHS-S group. The implications of physical exercise on leptin circulating levels have been shown to be depend on the intensity and duration of the exercise stimulus but usually contribute to decreased levels of this hormone in the plasma, accompanied by a decrease in body weight<sup>56</sup>. Although we did not detect significant alteration in the weight of the females, a decreasing tendency in body weight was observed during exercise protocols. A study in male Sprague-Dawley rats showed that although leptin was



maintained at decreased levels compared to the control group 6 weeks after a 12-week exercise protocol, the hormone levels increased significantly in the detraining period<sup>57</sup>. Nevertheless, the study was performed on male rats and the duration of the exercise intervention was longer than in the present study. The alterations induced by exercise on adiponectin and leptin circulating levels, even after physical exercise cessation, seem to be beneficial and, in fact, constituted relevant features according to the linear projection performed. Impaired glucose tolerance is one of the parameters used to assess metabolic dysfunction<sup>36</sup>. In this study, the animals fed with the HFHS diet showed higher glucose intolerance performed before beginning the exercise protocol. Interestingly, the capillary glucose levels evaluated at euthanasia revealed similar glucose levels between the experimental groups, although a higher median is observed in the HFHS-S group. The tail prick test was performed after overnight fasting which could influence the levels of glucose detected in the blood in non-diabetic animals. Fasting glucose is one of the parameters evaluated to aid the pre-diabetes and diabetes diagnosis, usually combined with other blood parameters, such as the glycated hemoglobin (HbA<sub>1c</sub>)<sup>58</sup>. Nevertheless, the objective of using the HFHS diet in this study was not to induce diabetes but to cause a metabolic imbalance.

Alterations in glucose homeostasis and hormonal levels can lead to a systemic inflammatory response which can affect the heart, resulting in cardiac inflammation<sup>52</sup>. A cardiac inflammatory state contributes to increased extracellular matrix (ECM) in the myocardium. Alterations in the cardiac ECM and dysregulation of its homeostasis lead to cardiac fibrosis and consequent cardiac dysfunction in aged and diabetic hearts<sup>59,60</sup>. The primary component of the ECM is collagen<sup>59</sup>. This study detected a slight increase in collagen fibers in the histological analysis of the HFHS-S and HFHS-E female hearts. These alterations did not seem to be induced by an inflammatory response within the myocardium since similar levels of proteins related to cardiac damage (cardiac Troponin T) and inflammation (IL-6 and TNF $\alpha$ ) were detected. Nevertheless, a decrease in collagen deposition was expected in response to exercise as an adaptation of cardiac remodeling, and since physiological cardiac hypertrophy does not usually contribute to exacerbated deposition of collagen fibers in the cardiac ECM, despite the expansion of the interstitial mesenchyme may also present as an adaptation to exercise. Indeed, the cardiac fibrosis induced by a high-fat diet was prevented by a 8-week exercise protocol in female C57BL/6J mice<sup>61</sup> and similar results were achieved in the hearts of aged rats<sup>62</sup>. Whether the slightly increased collagen deposition we observed in the hearts of exercised females is a consequence of detraining or not still needs to be assessed.

Alterations in glucose levels and in the inflammatory response are often associated with variations in the levels of circulating proteins. Therefore, we evaluated the effects of the HFHS diet and exercise cessation on various plasma parameters. Increased IGF-1 levels rise the risk of disease development, including metabolic diseases due to induced insulin resistance<sup>63</sup>. On the other hand, other studies show that IGF-1 deficiency might as well contribute to the same conditions<sup>64</sup>. Given this, the tight control of this hormone is crucial for balanced metabolic homeostasis. In our study, the plasma IGF-1 levels of sedentary female rats subjected to the HFHS were diminished, suggesting further metabolic dysfunction with possible implications for insulin signaling. The PI3K/Akt pathway is the central pathway associated with insulin signaling and can be activated by IGF-1. Lower levels of activated (phosphorylated) Akt can result from impaired insulin signaling in a state of insulin resistance. On the other hand, Akt overactivation can denote a mild physiological state of cardiac adaptation, e.g. as a feedback response to a previous insulin-resistant state possibly representing a mechanism of pathology origin, albeit it is also associated with the cardiac physiologic enlargement induced by exercise<sup>65</sup>. An increase of the ratio between the phosphorylated levels of Akt at the residue Ser 473 to total Akt was observed in this study. However, this result, together with the increased levels of phosphorylated P70 in the hearts of

exercised females might constitute an indication of previous cardiac adaptation to exercise. Activation of Akt/mammalian target of rapamycin (mTOR) signaling has been implicated in the exercise-induced cardiac hypertrophic response in diet-induced obese rats with concomitantly reduced insulin resistance<sup>66</sup>.

Cardiac metabolic flexibility maintenance is crucial to guarantee cardiac function and homeostasis, and it may be regulated by physiological conditions depending on the organism's environment. In various tissues, including the heart, hyperglycemia may induce hypoxia<sup>67</sup>. Additionally, hypoxia is induced by exercise to stimulate angiogenesis in the skeletal muscle and heart<sup>68</sup>. The low oxygen availability obligates cardiomyocytes to adapt by shifting metabolism to lower oxygen tension. This hypoxic state induces upregulation of HIF-1 $\alpha$  to increase glycolytic activity<sup>69</sup>. The transcript levels of HIF-1 $\alpha$  were elevated in the hearts of diabetic rats<sup>46</sup> and in treadmill-trained male mice<sup>68</sup>. Moreover, the relationship between increased HIF-1 $\alpha$  and decreased PPAR $\alpha$  expression has been established and linked to the return to a "fetal-like" phenotype usually observed in the failing heart<sup>70</sup>. The observed increased *Hif1 $\alpha$*  transcript levels in the hearts of exercised females and the decreased *Ppara* transcript levels are in line with the "fetal-like" phenotype. Yet, *Acox1* transcript levels, also involved in fatty acid oxidation, were tendentially increased in the hearts of the exercised females. Nevertheless, these results suggest that HIF-1 $\alpha$  signaling may constitute an adaptation to exercise despite the HFHS diet consumption. Alterations in the levels of PPAR $\alpha$  have been related to loss of cardiac metabolic flexibility<sup>71</sup>. Cardiac metabolic flexibility is governed by the energy state of cardiomyocytes<sup>45</sup>. The protein AMPK is responsible for the coordination of a general metabolic regulation to respond to the altered cardiac energy status, stimulating catabolic processes for ATP production and slowing anabolic ATP-consuming pathways<sup>72</sup>. We observed that exercise contributed to an increased ratio of phosphorylated AMPK to total protein, suggesting that exercise-induced metabolic alterations even after exercise cessation and with the consumption of the HFHS diet led to a consequent stimulation of AMPK functions so the heart can adapt to the new environment. Although these results should be indicative of a metabolic shift, which would result in altered activity of enzymes involved in glucose metabolism, that effect was not observed in the activity of the enzymes evaluated. Understanding substrate utilization in the hearts of these females deserves further studies.

Mitochondria are extremely important organelles that sustain cardiac contractility, and normal function through energy production in cardiomyocytes. In the heart, mitochondria play a critical role maintaining cardiac metabolic flexibility since this process molecularly relies on the interplay of metabolic pathways regulated by specific enzymes and transcription factors that interact with mitochondria<sup>73</sup>. Assessment of mitochondrial bioenergetics allows the evaluation of mitochondrial efficiency in response to physiological and pathological conditions. Regarding both complex-I and complex-II substrate-driven mitochondrial respiration, isolated cardiac mitochondria from female rats subjected to exercise showed an increased mitochondrial state 2 and ADP-induced membrane depolarization, which suggests these mitochondria were operating in an increased basal capacity. Preliminary electron microscopy data from our group revealed that the hearts of exercised females on the HFHS diet had a greater mitochondrial abundance, which present as smaller and denser structures. The observed increased ADP-induced membrane depolarization in the HFHS-S group of this study in the presence of succinate may be an early consequence of diet overload that may lead to increased OXPHOS, that later worsens. Furthermore, complex-I supported mitochondrial respiration showed impaired coupling between substrate oxidation and ADP phosphorylation, indicated by decreased RCR values. A decrease in RCR values is usually associated with decreased state 3 respiratory rates in the context of heart failure and western-diet consumption<sup>74</sup>, which is reversed by exercise<sup>75</sup>. However, cardiac

mitochondria from the detrained female rats of the present study did not show alterations in mitochondrial state 3 respiration but revealed higher state 4 respiration, which contributed to the observed lower RCR values. An increased state 4 respiration rate might be a consequence of intrinsic proton leak or intrinsic ATP hydrolysis activity. In fact, one study associated increased mitochondrial swelling with increased proton leak (higher state 4 mitochondrial respiration rates) in the hearts of rats exposed to ischemia and early reperfusion<sup>76</sup>. Moreover, exercise-induced state 4 increases were related to increased expression of the uncoupling protein 2 (UCP2) in male Sprague-Dawley rats<sup>77</sup>, while other studies report a hyperglycemia-induced reduced UCP2 expression in male Wistar rats<sup>78</sup>. However, while cardiac mitochondria of female rats exposed to the HFHS diet and a sedentary lifestyle presented lower mitochondrial efficiency when complex-I substrates were used, with decreased RCR values and needing more oxygen to phosphorylate the same amount of ADP (presented by the decreased ADP/O values), without increased basal respiration and significant changes in state 3 or state 4 respiration rates, exercise, even after a cessation period, seemed to induce an adaptative response in the heart that prevails at least 8 weeks after exercise.

To understand if the observed response is induced by an increase in mitochondria number, we assessed several mitochondrial biomarkers. The protein POLRMT is responsible for the transcription of the circular mammalian mtDNA and is indispensable for mtDNA replication<sup>47</sup>. The cardiac levels of this transcript were decreased in the hearts of females subjected to the HFHS diet independently of exercise. Although conditional knock-out of this gene leads to severe mitochondrial dysfunction in mice, the exact cardiac repercussions of the alterations in its regulation are unknown<sup>47</sup>. Despite that, it has been observed that absence of POLRMT results in increased free-TFAM pool<sup>47</sup>. Nevertheless, this study showed no alterations regarding proteins involved in mitochondrial biogenesis or dynamic (fission and fusion) processes. Based on our preliminary observations of the mitochondrial structures in the females' hearts, we raised the possibility that some of the molecular alterations that might have been induced by exercise while on the HFHS diet may no longer occurring in the heart at 25 weeks of age, 8 weeks after exercise cessation.

The contribution of high-fat and high-fat, high-sucrose diets to mitochondrial impairments in the heart includes decreased ATP levels in the cardiac tissue<sup>79,80</sup> and cardiac mitochondria<sup>81</sup>, as well as an increase in NADPH levels<sup>82</sup>. Exercise has been shown to beneficially impact these diet-induced effects<sup>23</sup>. In the present study, the cardiac mitochondrial fraction of females subjected to the HFHS diet during the experiment, showed decreased mitochondrial ATP levels and increased mitochondrial NAD(P)H levels, consistent with previous studies. Even a short exercise period prevented these alterations in cardiac mitochondria. The important role of Nrf2 when mitochondrial oxidative phosphorylation efficacy is decreased and consequent mitochondrial dysfunction occurs and in CVD has been extensively reported<sup>83,84</sup>, as well as its beneficial role in response to exercise for cardiac function<sup>25</sup>. Nrf2 knockdown results in decreased ATP levels while Keap1 knockdown, the protein involved in the tight regulation of Nrf2 activity, leads to increased ATP levels<sup>83</sup>. In this work, only the hearts of females engaged in the exercise protocol while fed with the HFHS diet showed increased Nrf2 protein levels, compared to both the control and HFHS-S groups. This exercise-induced adaptation, which prevails 8-weeks after exercise cessation, might explain the normalized levels of ATP and NAD(P)H in cardiac mitochondria of exercised females, and denote the lack of an adaptative response in the HFHS-S hearts that also showed reduced mitochondrial efficiency. Given that these alterations might be a consequence of increased reactive oxygen species (ROS) levels, and the role of complex III in ROS production, which increased levels are related to UQCRC2 deficiency<sup>85</sup>, the increase of mitochondrial complex III subunit UQCRC2 protein levels observed in this study may indicate a previous

adaptation induced by exercise. Whenever ROS production is augmented, the antioxidant defense systems take action to prevent further damage. Nrf2 is involved in the transcription of several genes that encode proteins involved in antioxidant defenses, playing a crucial role in redox balance<sup>41</sup>. Nrf2 directly regulates the expression of GPX4, SOD1, and catalase<sup>51</sup>. Indeed, in this study, the levels of GPX4 were significantly increased in the hearts of previously exercised females, and a similar behavior was observed in SOD1 protein levels, and the catalase activity increase was more evident in the hearts of females subjected to exercise and subsequent exercise cessation. These results are undoubtedly adaptations induced by the short-period exercise intervention that prevail at the 8<sup>th</sup> week of exercise cessation.

## Conclusions

Animal studies designed to model human diseases often exclude female subjects, which limits our understanding of disease mechanisms and potential interventions that may be specific for females. Our study focused on the effects of short-term exercise and subsequent cessation on cardiac tissue and mitochondrial function in female rats fed a high-fat, high-sugar (HFHS) diet. We found that the HFHS diet alone, and exercise followed by cessation on the HFHS diet, had significant impacts on mitochondrial parameters, including bioenergetics, ATP and NAD(P)H levels, and redox balance. Our results suggest that the transcription factor Nrf2 may play a role in adaptive cardiac responses to exercise even after short-term intervention and exercise cessation. However, the overall impact of these adaptations on whole-heart metabolic function remains to be fully elucidated. Our approach to dietary and exercise intervention closely mirrors the lifestyle of many individuals in Western countries, where high-caloric diets and physical inactivity are common and may thus provide valuable insights into disease mechanisms and potential interventions for this population.

## References

1. Tsao CW, Aday AW, Almarzooq ZI, Alonso A, Beaton AZ, Bittencourt MS, Boehme AK, Buxton AE, Carson AP, Commodore- Mensah Y, Elkind MSV, Evenson KR, Eze-Nliam C, Ferguson JF, Generoso G, Ho JE, Kalani R, Khan SS, Kissela BM, Knutson KL, Levine DA, Lewis TT, MS on behalf of the AHAC on E and PSC and SS. Heart disease and stroke statistics—2022 update: a report from the American Heart Association. *Circulation*. 2022;(145):e153–e639. doi:10.1161/CIR.0000000000001052
2. Geraghty L, Figtree GA, Schutte AE, Patel S, Woodward M, Arnott C. Cardiovascular Disease in Women: From Pathophysiology to Novel and Emerging Risk Factors. *Heart Lung Circ*. 2021;30(1):9-17. doi:10.1016/j.hlc.2020.05.108
3. Vogel B, Acevedo M, Appelman Y, et al. The Lancet women and cardiovascular disease Commission: reducing the global burden by 2030. *Lancet*. 2021;397(10292):2385-2438. doi:10.1016/S0140-6736(21)00684-X
4. Norris CM, Yip CYY, Nerenberg KA, et al. State of the Science in Women's Cardiovascular Disease: A Canadian Perspective on the Influence of Sex and Gender. *J Am Heart Assoc*. 2020;9(4). doi:10.1161/JAHA.119.015634
5. Woodward M. Cardiovascular disease and the female disadvantage. *Int J Environ Res Public Health*. 2019;16(7). doi:10.3390/ijerph16071165
6. Diniz MS, Tocantins C, Grilo LF, Pereira SP. The Bitter Side of Sugar Consumption: A

- Mitochondrial Perspective on Diabetes Development. *Diabetology*. 2022;3(4):583-595. doi:10.3390/diabetology3040044
7. Hunter I, Soler A, Joseph G, et al. Cardiovascular function in male and female JCR:LA-cp rats: Effect of high-fat/high-sucrose diet. *Am J Physiol - Hear Circ Physiol*. 2017;312(4):H742-H751. doi:10.1152/ajpheart.00535.2016
  8. Pereira-Silva DC, Machado-Silva RP, Castro-Pinheiro C, Fernandes-Santos C. Does gender influence cardiovascular remodeling in C57BL/6J mice fed a high-fat, high-sucrose and high-salt diet? *Int J Exp Pathol*. 2019;100(3):153-160. doi:10.1111/iep.12318
  9. Maurya SK, Carley AN, Maurya CK, Lewandowski ED. Western Diet Causes Heart Failure With Reduced Ejection Fraction and Metabolic Shifts After Diastolic Dysfunction and Novel Cardiac Lipid Derangements. *JACC Basic to Transl Sci*. 2023. doi:10.1016/j.jacbts.2022.10.009
  10. Stewart RAH, Wallentin L, Benatar J, et al. Dietary patterns and the risk of major adverse cardiovascular events in a global study of high-risk patients with stable coronary heart disease. *Eur Heart J*. 2016;37(25):1993-2001. doi:10.1093/eurheartj/ehw125
  11. Pettman TL, Buckley JD, Misan GMH, Coates AM, Howe PRC. Health benefits of a 4-month group-based diet and lifestyle modification program for individuals with metabolic syndrome. *Obes Res Clin Pract*. 2009. doi:10.1016/j.orcp.2009.06.002
  12. Lin X, Zhang X, Guo J, et al. Effects of Exercise Training on Cardiorespiratory Fitness and. 2015:1-28. doi:10.1161/JAHA.115.002014
  13. Sun S, Zhang H, Kong Z, Shi Q, Tong TK. Twelve weeks of low volume sprint interval training improves cardio-metabolic health outcomes in overweight females. *J Sports Sci*. 2019;37(11):1257-1264. doi:10.1080/02640414.2018.1554615
  14. Slentz CA, Bateman LA, Willis LH, et al. Effects of exercise training alone vs a combined exercise and nutritional lifestyle intervention on glucose homeostasis in prediabetic individuals : a randomised controlled trial. *Diabetologia*. 2016. doi:10.1007/s00125-016-4051-z
  15. Hivert MF, Arena R, Forman DE, et al. Medical Training to Achieve Competency in Lifestyle Counseling: An Essential Foundation for Prevention and Treatment of Cardiovascular Diseases and Other Chronic Medical Conditions: A Scientific Statement from the American Heart Association. *Circulation*. 2016;134(15):e308-e327. doi:10.1161/CIR.0000000000000442
  16. Arena R, Lavie CJ, Hivert MF, Williams MA, Briggs PD, Guazzi M. Who will deliver comprehensive healthy lifestyle interventions to combat non-communicable disease? Introducing the healthy lifestyle practitioner discipline. *Expert Rev Cardiovasc Ther*. 2016;14(1):15-22. doi:10.1586/14779072.2016.1107477
  17. Nolan PB, Keeling SM, Robitaille CA, Buchanan CA, Dalleck LC. The effect of detraining after a period of training on cardiometabolic health in previously sedentary individuals. *Int J Environ Res Public Health*. 2018;15(10). doi:10.3390/ijerph15102303
  18. Tofas T, Draganidis D, Deli CK, Georgakouli K, Fatouros IG, Jamurtas AZ. Exercise-induced regulation of redox status in cardiovascular diseases: The role of exercise training and detraining. *Antioxidants*. 2020;9(1):1-41. doi:10.3390/antiox9010013
  19. Leitão L, Pereira A, Mazini M, et al. Effects of three months of detraining on the health profile of older women after a multicomponent exercise program. *Int J Environ Res Public Health*. 2019;16(20):2-11. doi:10.3390/ijerph16203881

20. Carneiro-Júnior MA, Quintão-Júnior JF, Drummond LR, et al. The benefits of endurance training in cardiomyocyte function in hypertensive rats are reversed within four weeks of detraining. *J Mol Cell Cardiol.* 2013;57(1):119-128. doi:10.1016/j.yjmcc.2013.01.013
21. Chatterjee E, Chaudhuri RD, Sarkar S. Cardiomyocyte targeted overexpression of IGF1 during detraining restores compromised cardiac condition via mTORC2 mediated switching of PKC $\delta$  to PKC $\alpha$ . *Biochim Biophys Acta - Mol Basis Dis.* 2019;1865(10):2736-2752. doi:10.1016/j.bbadis.2019.07.003
22. Kanaan GN, Harper ME. Cellular redox dysfunction in the development of cardiovascular diseases. *Biochim Biophys Acta - Gen Subj.* 2017;1861(11):2822-2829. doi:10.1016/j.bbagen.2017.07.027
23. Wang SY, Zhu S, Wu J, et al. Exercise enhances cardiac function by improving mitochondrial dysfunction and maintaining energy homeostasis in the development of diabetic cardiomyopathy. *J Mol Med.* 2020;98(2):245-261. doi:10.1007/s00109-019-01861-2
24. Kavazis AN, McClung JM, Hood DA, Powers SK. Exercise induces a cardiac mitochondrial phenotype that resists apoptotic stimuli. *Am J Physiol - Hear Circ Physiol.* 2008;294(2):928-935. doi:10.1152/ajpheart.01231.2007
25. Vasanthi R, Muthusamy, Sankaranarayanan Kannanb, Kamal Sadhaasivama, Sellamuthu S, Goundera, Christopher J, Davidsona, Christoph Boehemec, John R. Hoidal, Li Wang and NSR. Acute exercise stress activates Nrf2/ARE signaling and promotes antioxidant mechanisms in the myocardium. *Free Radic Biol Med.* 2012;52(2):366-376. doi:10.1016/j.freeradbiomed.2011.10.440.Acute
26. Stevanović-Silva J, Beleza J, Coxito P, et al. Maternal high-fat high-sucrose diet and gestational exercise modulate hepatic fat accumulation and liver mitochondrial respiratory capacity in mothers and male offspring. *Metabolism.* 2021;116:154704. doi:10.1016/j.metabol.2021.154704
27. Zhang L, Zhang L. Voluntary oral administration of drugs in mice. *Protoc Exch.* 2011:1-8. doi:10.1038/protex.2011.236
28. Pereira GC, Pereira SP, Pereira FB, et al. *Early Cardiac Mitochondrial Molecular and Functional Responses to Acute Anthracycline Treatment in Wistar Rats.* Vol 169.; 2019. doi:10.1093/toxsci/kfz026
29. Pereira SP, Santos SMA, Fernandes MAS, et al. Improving pollutants environmental risk assessment using a multi model toxicity determination with in vitro, bacterial, animal and plant model systems: The case of the herbicide alachlor. *Environ Pollut.* 2021;286. doi:10.1016/j.envpol.2021.117239
30. Grilo LF, Martins JD, Cavallaro CH, Nathanielsz PW, Oliveira PJ, Pereira SP. Development of a 96-well based assay for kinetic determination of catalase enzymatic activity in biological samples. *Toxicol Vitro.* 2020;69(May):104996. doi:10.1016/j.tiv.2020.104996
31. Gupte SA, Levine RJ, Gupte RS, et al. Glucose-6-phosphate dehydrogenase-derived NADPH fuels superoxide production in the failing heart. *J Mol Cell Cardiol.* 2006;41(2):340-349. doi:10.1016/j.yjmcc.2006.05.003
32. Crabtree B, Newsholme EA. The activities of phosphorylase, hexokinase, phosphofructokinase, lactate dehydrogenase and the glycerol 3-phosphate dehydrogenases in muscles from vertebrates and invertebrates. *Biochem J.* 1972;126(1):49-58. doi:10.1042/bj1260049
33. Malfitano C, de Souza Junior AL, Carbonaro M, et al. Glucose and fatty acid

- metabolism in infarcted heart from streptozotocin-induced diabetic rats after 2 weeks of tissue remodeling. *Cardiovasc Diabetol*. 2015;14(1):1-10. doi:10.1186/s12933-015-0308-y
34. Decker T, Lohmann-Matthes ML. A quick and simple method for the quantitation of lactate dehydrogenase release in measurements of cellular cytotoxicity and tumor necrosis factor (TNF) activity. *J Immunol Methods*. 1988;115(1):61-69. doi:10.1016/0022-1759(88)90310-9
  35. Klitgaard HB, Kilbak JH, Nozawa EA, Seidel A V., Magkos F. Physiological and Lifestyle Traits of Metabolic Dysfunction in the Absence of Obesity. *Curr Diab Rep*. 2020;20(6). doi:10.1007/s11892-020-01302-2
  36. Bellissimo MP, Cai Q, Ziegler TR, et al. Plasma High-Resolution Metabolomics Differentiates Adults with Normal Weight Obesity from Lean Individuals. *Obesity*. 2019;27(11):1729-1737. doi:10.1002/oby.22654
  37. Chait A, den Hartigh LJ. Adipose Tissue Distribution, Inflammation and Its Metabolic Consequences, Including Diabetes and Cardiovascular Disease. *Front Cardiovasc Med*. 2020;7(February):1-41. doi:10.3389/fcvm.2020.00022
  38. Ma ZG, Yuan YP, Wu HM, Zhang X, Tang QZ. Cardiac fibrosis: New insights into the pathogenesis. *Int J Biol Sci*. 2018;14(12):1645-1657. doi:10.7150/ijbs.28103
  39. Zheng H, Yang Z, Xin Z, et al. Glycogen synthase kinase-3 $\beta$ : A promising candidate in the fight against fibrosis. *Theranostics*. 2020;10(25):11737-11753. doi:10.7150/thno.47717
  40. De Rosa S, Arcidiacono B, Chiefari E, Brunetti A, Indolfi C, Foti DP. Type 2 diabetes mellitus and cardiovascular disease: Genetic and epigenetic links. *Front Endocrinol (Lausanne)*. 2018;9(JAN):1-13. doi:10.3389/fendo.2018.00002
  41. Da Costa RM, Rodrigues D, Pereira CA, et al. Nrf2 as a potential mediator of cardiovascular risk in metabolic diseases. *Front Pharmacol*. 2019;10(APR):1-12. doi:10.3389/fphar.2019.00382
  42. Ormazabal V, Nair S, Elfeky O, Aguayo C, Salomon C, Zuñiga FA. Association between insulin resistance and the development of cardiovascular disease. *Cardiovasc Diabetol*. 2018;17(1):1-14. doi:10.1186/s12933-018-0762-4
  43. Bartlett J, Trivedi P, Pulinilkunnill T. *Insulin Signaling in Cardiac Health and Disease*. Elsevier Inc.; 2017. doi:10.1016/B978-0-12-803111-7.00012-9
  44. Hue L, Beauloye C, Bertrand L. *Principles in the Regulation of Cardiac Metabolism*. Elsevier Inc.; 2016. doi:10.1016/b978-0-12-802394-5.00005-4
  45. Karwi QG, Uddin GM, Ho KL, Lopaschuk GD. Loss of Metabolic Flexibility in the Failing Heart. *Front Cardiovasc Med*. 2018;5(June):1-19. doi:10.3389/fcvm.2018.00068
  46. Cerychova R, Pavlinkova G. HIF-1, metabolism, and diabetes in the embryonic and adult heart. *Front Endocrinol (Lausanne)*. 2018;9(AUG):1-14. doi:10.3389/fendo.2018.00460
  47. Kühn I, Miranda M, Posse V, et al. POLRMT regulates the switch between replication primer formation and gene expression of mammalian mtDNA. *Sci Adv*. 2016;2(8):1-14. doi:10.1126/sciadv.1600963
  48. Vásquez-Trincado C, García-Carvajal I, Pennanen C, et al. Mitochondrial dynamics, mitophagy and cardiovascular disease. *J Physiol*. 2016;594(3):509-525. doi:10.1113/JP271301

49. Chistiakov DA, Shkurat TP, Melnichenko AA, Grechko A V., Orekhov AN. The role of mitochondrial dysfunction in cardiovascular disease: a brief review. *Ann Med*. 2018;50(2):121-127. doi:10.1080/07853890.2017.1417631
50. Zhou B, Tian R. Mitochondrial dysfunction in pathophysiology of heart failure. *J Clin Invest*. 2018;128(9):3716-3726. doi:10.1172/JCI120849
51. Chen QM, Maltagliati AJ. Nrf2 at the heart of oxidative stress and cardiac protection. *Physiol Genomics*. 2018;50(2):77-97. doi:10.1152/physiolgenomics.00041.2017
52. Zhao S, Kusminski CM, Scherer PE. Adiponectin, Leptin and Cardiovascular Disorders. *Circ Res*. 2021;128(1):136-149. doi:10.1161/CIRCRESAHA.120.314458
53. Grilo LF, Diniz MS, Tocantins C, Areia AL, Pereira SP. The Endocrine–Metabolic Axis Regulation in Offspring Exposed to Maternal Obesity—Cause or Consequence in Metabolic Disease Programming? *Obesities*. 2022;2(3):236-255. doi:10.3390/obesities2030019
54. Aslam M, Madhu S V. Development of metabolic syndrome in high-sucrose diet fed rats is not associated with decrease in adiponectin levels. *Endocrine*. 2017;58(1):59-65. doi:10.1007/s12020-017-1403-5
55. Moreno-Fernández S, Garcés-Rimón M, Vera G, Astier J, Landrier JF, Miguel M. High fat/high glucose diet induces metabolic syndrome in an experimental rat model. *Nutrients*. 2018;10(10):1-15. doi:10.3390/nu10101502
56. Hulver MW, Houmard JA. Plasma leptin and exercise: Recent findings. *Sport Med*. 2003;33(7):473-482. doi:10.2165/00007256-200333070-00001
57. Jang JH, Joo CH. The Effects of Training and Detraining on Metabolic Hormones in Rats. *Exerc Sci*. 2017;26(2):139-144. doi:10.15857/ksep.2017.26.2.139
58. Bancks MP, Ning H, Allen NB, et al. Long-term absolute risk for cardiovascular disease stratified by fasting glucose level. *Diabetes Care*. 2019;42(3):457-465. doi:10.2337/dc18-1773
59. Kwak H-B. Aging, exercise, and extracellular matrix in the heart. *J Exerc Rehabil*. 2013;9(3):338-347. doi:10.12965/jer.130049
60. Wilson AJ, Gill EK, Abudalo RA, Edgar KS, Watson CJ, Grieve DJ. Reactive oxygen species signalling in the diabetic heart: Emerging prospect for therapeutic targeting. *Heart*. 2018;104(4):293-299. doi:10.1136/heartjnl-2017-311448
61. Kesharwani V, Chavali V, Hackfort BT, Tyagi SC, Mishra PK. Exercise ameliorates high fat diet induced cardiac dysfunction by increasing interleukin 10. *Front Physiol*. 2015;6(APR):1-7. doi:10.3389/fphys.2015.00124
62. Kwak H, Kim J, Joshi K, Yeh A, Martinez DA, Lawler JM. Exercise training reduces fibrosis and matrix metalloproteinase dysregulation in the aging rat heart. *FASEB J*. 2011;25(3):1106-1117. doi:10.1096/fj.10-172924
63. Hill CM, Arum O, Boparai RK, et al. Female PAPP-A knockout mice are resistant to metabolic dysfunction induced by high-fat/high-sucrose feeding at middle age. *Age (Omaha)*. 2015;37(3):1-14. doi:10.1007/s11357-015-9765-1
64. Aguirre GA, Ita JR, Garza RG, Castilla-Cortazar I. Insulin-like growth factor-1 deficiency and metabolic syndrome. *J Transl Med*. 2016;14(1):1-23. doi:10.1186/s12967-015-0762-z
65. Neri Serneri GG, Boddi M, Modesti PA, et al. Increased cardiac sympathetic activity and insulin-like growth factor-I formation are associated with physiological hypertrophy in



- athletes. *Circ Res*. 2001;89(11):977-982. doi:10.1161/hh2301.100982
66. Medeiros C, Frederico MJ, Da Luz G, et al. Exercise training reduces insulin resistance and upregulates the mTOR/p70S6k pathway in cardiac muscle of diet-induced obesity rats. *J Cell Physiol*. 2011;226(3):666-674. doi:10.1002/jcp.22387
  67. Huang Y Te, Liu CH, Yang YC, et al. ROS- and HIF1 $\alpha$ -dependent IGFBP3 upregulation blocks IGF1 survival signaling and thereby mediates high-glucose-induced cardiomyocyte apoptosis. *J Cell Physiol*. 2019;234(8):13557-13570. doi:10.1002/jcp.28034
  68. Bellafiore M, Battaglia G, Bianco A, Palma A. Expression pattern of angiogenic factors in healthy heart in response to physical exercise intensity. *Front Physiol*. 2019;10(March). doi:10.3389/fphys.2019.00238
  69. Belanger AJ, Luo Z, Vincent KA, et al. Hypoxia-inducible factor 1 mediates hypoxia-induced cardiomyocyte lipid accumulation by reducing the DNA binding activity of peroxisome proliferator-activated receptor  $\alpha$ /retinoid X receptor. *Biochem Biophys Res Commun*. 2007;364(3):567-572. doi:10.1016/j.bbrc.2007.10.062
  70. Vega RB, Konhilas JP, Kelly DP, Leinwand LA. Molecular Mechanisms Underlying Cardiac Adaptation to Exercise. *Cell Metab*. 2017;25(5):1012-1026. doi:10.1016/j.cmet.2017.04.025
  71. Montaigne D, Butruille L, Staels B. PPAR control of metabolism and cardiovascular functions. *Nat Rev Cardiol*. 2021;1. doi:10.1038/s41569-021-00569-6
  72. Li HL, Yin R, Chen D, et al. Long-term activation of adenosine monophosphate-activated protein kinase attenuates pressure-overload-induced cardiac hypertrophy. *J Cell Biochem*. 2007;100(5):1086-1099. doi:10.1002/jcb.21197
  73. Vujic A, Koo ANM, Prag HA, Krieg T. Mitochondrial redox and TCA cycle metabolite signaling in the heart. *Free Radic Biol Med*. 2021;166(March):287-296. doi:10.1016/j.freeradbiomed.2021.02.041
  74. Neves FA, Cortez E, Bernardo AF, et al. Heart energy metabolism impairment in Western-diet induced obese mice. *J Nutr Biochem*. 2014;25(1):50-57. doi:10.1016/j.jnutbio.2013.08.014
  75. Phielix E, Meex R, Moonen-Kornips E, Hesselink MKC, Schrauwen P. Exercise training increases mitochondrial content and ex vivo mitochondrial function similarly in patients with type 2 diabetes and in control individuals. *Diabetologia*. 2010;53(8):1714-1721. doi:10.1007/s00125-010-1764-2
  76. Bosetti F, Baracca A, Lenaz G, Solaini G. Increased state 4 mitochondrial respiration and swelling in early post-ischemic reperfusion of rat heart. *FEBS Lett*. 2004;563(1-3):161-164. doi:10.1016/S0014-5793(04)00294-7
  77. Bo H, Jiang N, Ma G, et al. Regulation of mitochondrial uncoupling respiration during exercise in rat heart: Role of reactive oxygen species (ROS) and uncoupling protein 2. *Free Radic Biol Med*. 2008;44(7):1373-1381. doi:10.1016/j.freeradbiomed.2007.12.033
  78. Kutsche HS, Schreckenber R, Weber M, et al. Alterations in Glucose Metabolism During the Transition to Heart Failure: The Contribution of UCP-2. *Cells*. 2020;9(3):1-19. doi:10.3390/cells9030552
  79. Kang KW, Kim OS, Chin JY, et al. Diastolic dysfunction induced by a high-fat diet is associated with mitochondrial abnormality and adenosine triphosphate levels in rats. *Endocrinol Metab*. 2015;30(4):557-568. doi:10.3803/EnM.2015.30.4.557

80. Chen D, Li X, Zhang LT, Zhu M, Gao L. A high-fat diet impairs mitochondrial biogenesis, mitochondrial dynamics, and the respiratory chain complex in rat myocardial tissues. *J Cell Biochem.* 2018;119(11):9602. doi:10.1002/jcb.27068
81. Sverdlov AL, Elezaby A, Behring JB, et al. High fat, high sucrose diet causes cardiac mitochondrial dysfunction due in part to oxidative post-translational modification of mitochondrial complex II. *J Mol Cell Cardiol.* 2015;78:165-173. doi:10.1016/j.yjmcc.2014.07.018
82. Mayyas F, Alzoubi KH, Al-Taleb Z. Impact of high fat/high salt diet on myocardial oxidative stress. *Clin Exp Hypertens.* 2017;39(2):126-132. doi:10.1080/10641963.2016.1226894
83. Dinkova-Kostova AT, Abramov AY. The emerging role of Nrf2 in mitochondrial function. *Free Radic Biol Med.* 2015;88(Part B):179-188. doi:10.1016/j.freeradbiomed.2015.04.036
84. Vashi R, Patel BM. NRF2 in Cardiovascular Diseases: a Ray of Hope! *J Cardiovasc Transl Res.* 2021;14(3):573-586. doi:10.1007/s12265-020-10083-8
85. Shang Y, Zhang F, Li D, et al. Overexpression of UQCRC2 is correlated with tumor progression and poor prognosis in colorectal cancer. *Pathol Res Pract.* 2018;214(10):1613-1620. doi:10.1016/j.prp.2018.08.012

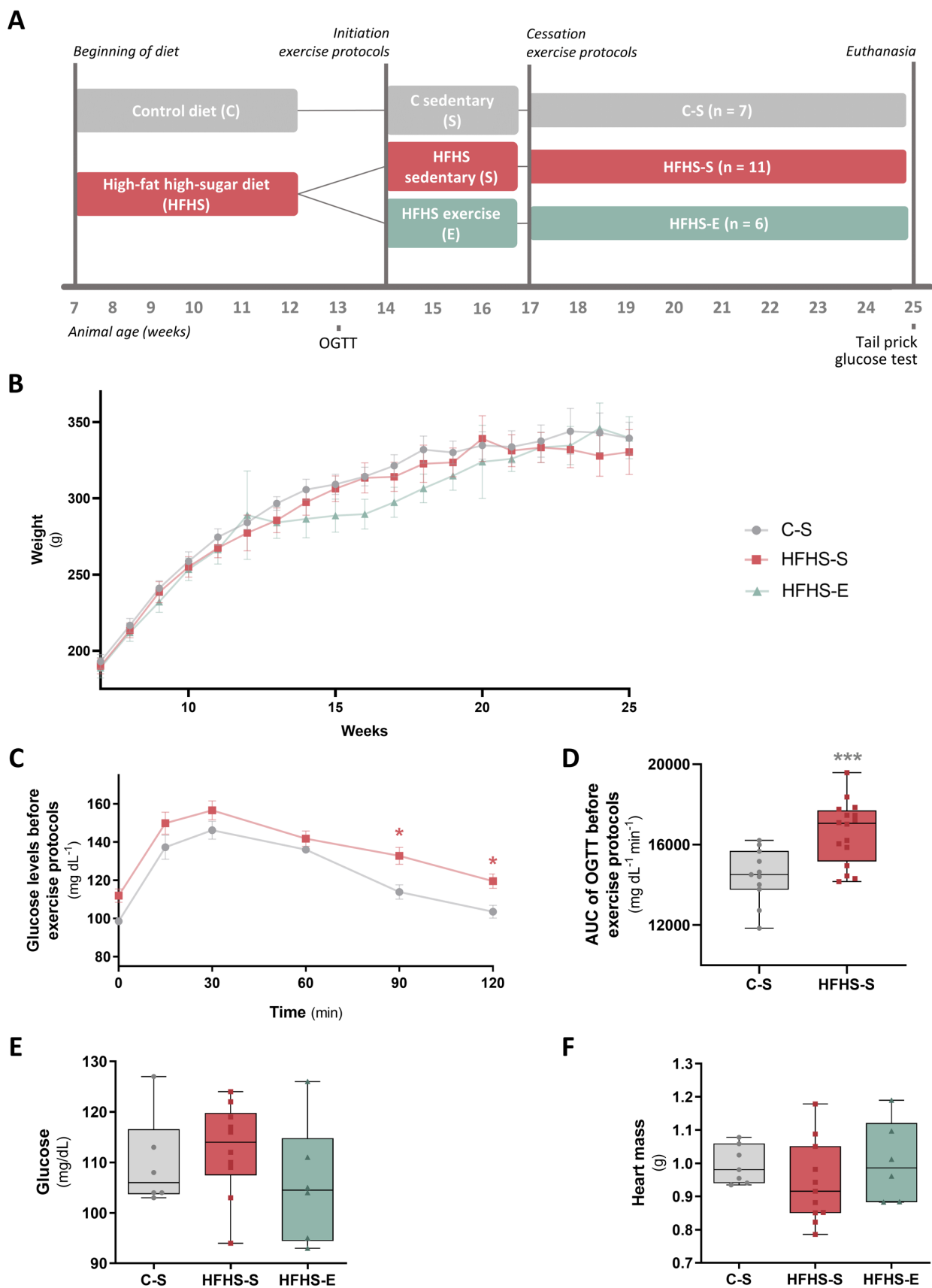


**Figure 1.** Model characterization. (A) Timeline of the experimental design used in the study. (B) Body weight variation of the female rats throughout the experimental protocol until reaching the 25 weeks of age. (C) OGTT performed before initiation of exercise protocols, at 13 weeks of age, and (D) respective area

under the curve (AUC). (E) Glucose levels assessed by the tail prick test at euthanasia (25 weeks of age). (F) Heart mass. The period of the exercise protocol (14 to 17 weeks) is represented by the light green shadow. Comparison between the experimental groups in the OGTTs (C and E) was performed using multiple t-tests corrected for multiple comparisons with the Holm Sidak method and for the AUC (D and F) with unpaired t-test when ANOVA  $p < 0.1$  and after confirming normality with the Shapiro-Wilk normality test. \*\*\*\*  $p < 0.0001$  HFHS-S vs C-S, \*\*\*\*  $p < 0.0001$  HFHS-E vs C-S, \*\*\*  $p < 0.001$  HFHS-S vs C-S, \*\*\*  $p < 0.001$  HFHS-E vs C-S, \*\*  $p < 0.01$  HFHS-S vs C-S, \*\*  $p < 0.01$  HFHS-E vs C-S, \*  $p < 0.05$  HFHS-S vs C-S. OGTT – oral glucose tolerance test.

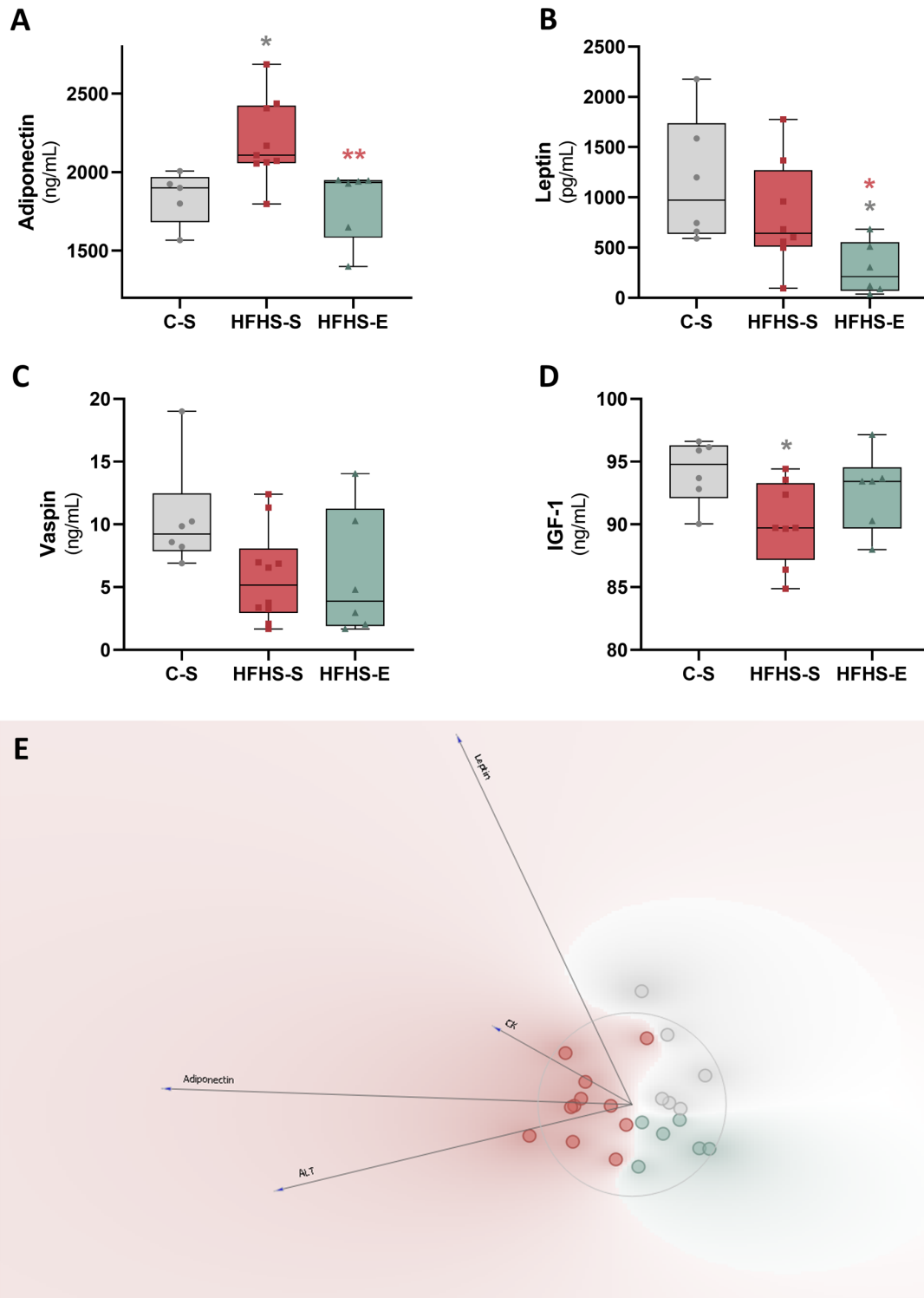
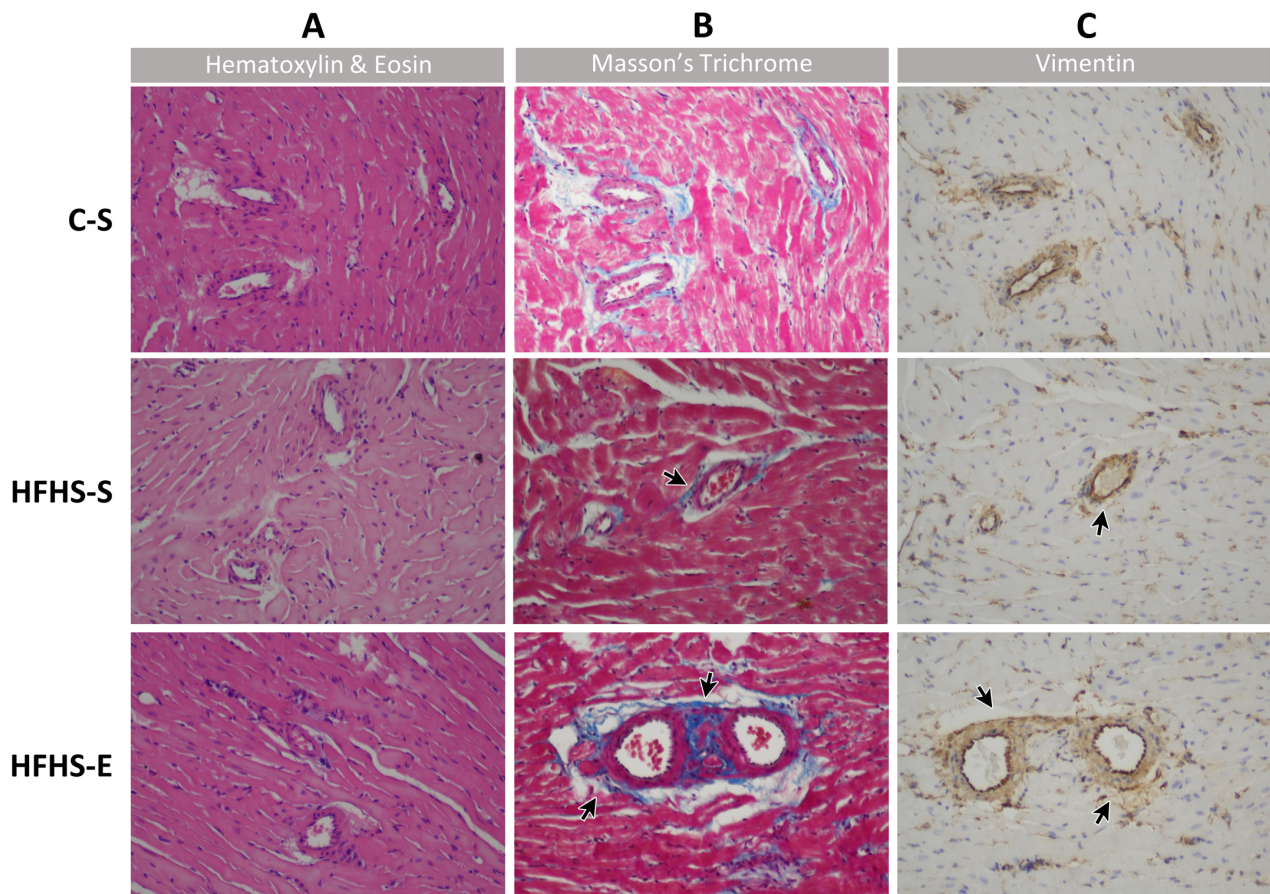


**Figure 2.** Plasma biochemical characterization of metabolic hormones: (A) adiponectin, (B) leptin, (C) vaspin, and (D) IGF-1 – insulin-like growth factor 1. (E) Linear projection revealing the most relevant plasma parameters to discriminate the experimental groups. ALT – alanine aminotransferase; CK - creatine kinase. \*\*  $p < 0.01$  HFHS-E vs HFHS-S, \*  $p < 0.05$  HFHS-S vs C-S or HFHS-E vs C-S, \*  $p < 0.05$  HFHS-E vs HFHS-S.



**D**

Protein levels of cardiac damage and inflammation markers.

	C-S	HFHS-S	HFHS-E
Cardiac troponin T	1.00 [0.796, 1.20]	0.784 [0.611, 1.44]	0.439 [0.216, 0.958]
IL-6	1.00 [0.638, 1.36]	0.963 [0.491, 1.50]	0.678 [0.351, 0.917]
TNF $\alpha$	1.00 [0.704, 1.30]	0.831 [0.422, 1.61]	0.351 [0.0400, 1.98]

**Figure 3.** Cardiac morphological characterization by histological analysis of the tissue. (A) Hematoxylin and eosin staining. (B) Masson's Trichrome staining. (C) Immunohistochemical staining using vimentin. Black arrows point to stronger stainings of the perivascular matrix or its elements. Amplification (x200). (D) Protein levels of cardiac damage (cardiac troponin T) and inflammation markers (IL-6 – interleukin 6 and TNF $\alpha$  – tumor necrosis factor  $\alpha$ ), evaluated by Western blot using heart tissue extracts. Data are represented as median [Q1, Q3]. Data were normalized to the average of C-S, considered = 1. C-S (n = 6); HFHS-S (n = 7), HFHS-E (n = 5).

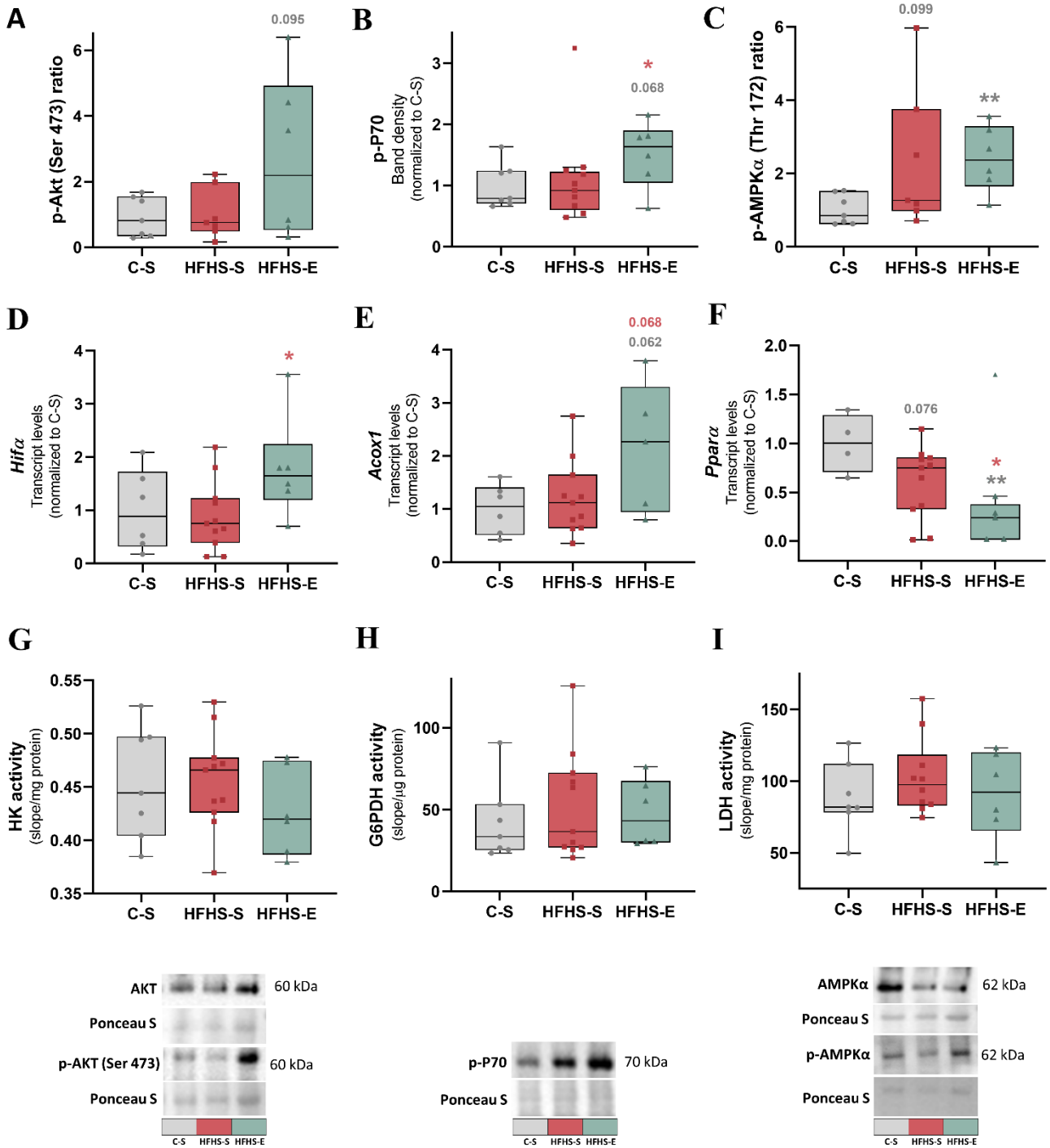


**Figure 4.** Modulation of cardiac metabolism plasticity by HFHS and exercise. Levels of proteins involved in the insulin signaling response, downstream target and related metabolic mechanisms evaluated by Western blot of cardiac tissue extracts: (A) p-Akt (Ser 473) to Akt ratio, (B) p-P70, (C) p-AMPK $\alpha$  (Thr 172) to AMPK $\alpha$  ratio. Levels of transcripts of (D) *Hif1 $\alpha$*  and transcripts related to  $\beta$ -oxidation: (E) *Acox1*, (F) *Ppara*; Enzymatic activity of proteins involved in glucose metabolism: (G) Hexokinase (HK), (H) Glucose-6-phosphate dehydrogenase (G6PDH), (I) Lactate dehydrogenase (LDH). Comparison between the experimental groups was performed using unpaired t test or Mann-Whitney when one-way ANOVA  $p < 0.1$  and confirming normality with the Shapiro-Wilk normality test. \*  $p < 0.05$  HFHS-E vs HFHS-S, \*\*  $p < 0.01$  HFHS-E vs C-S. Western blotting and PCR data were normalized to the average of C-S, considered = 1.

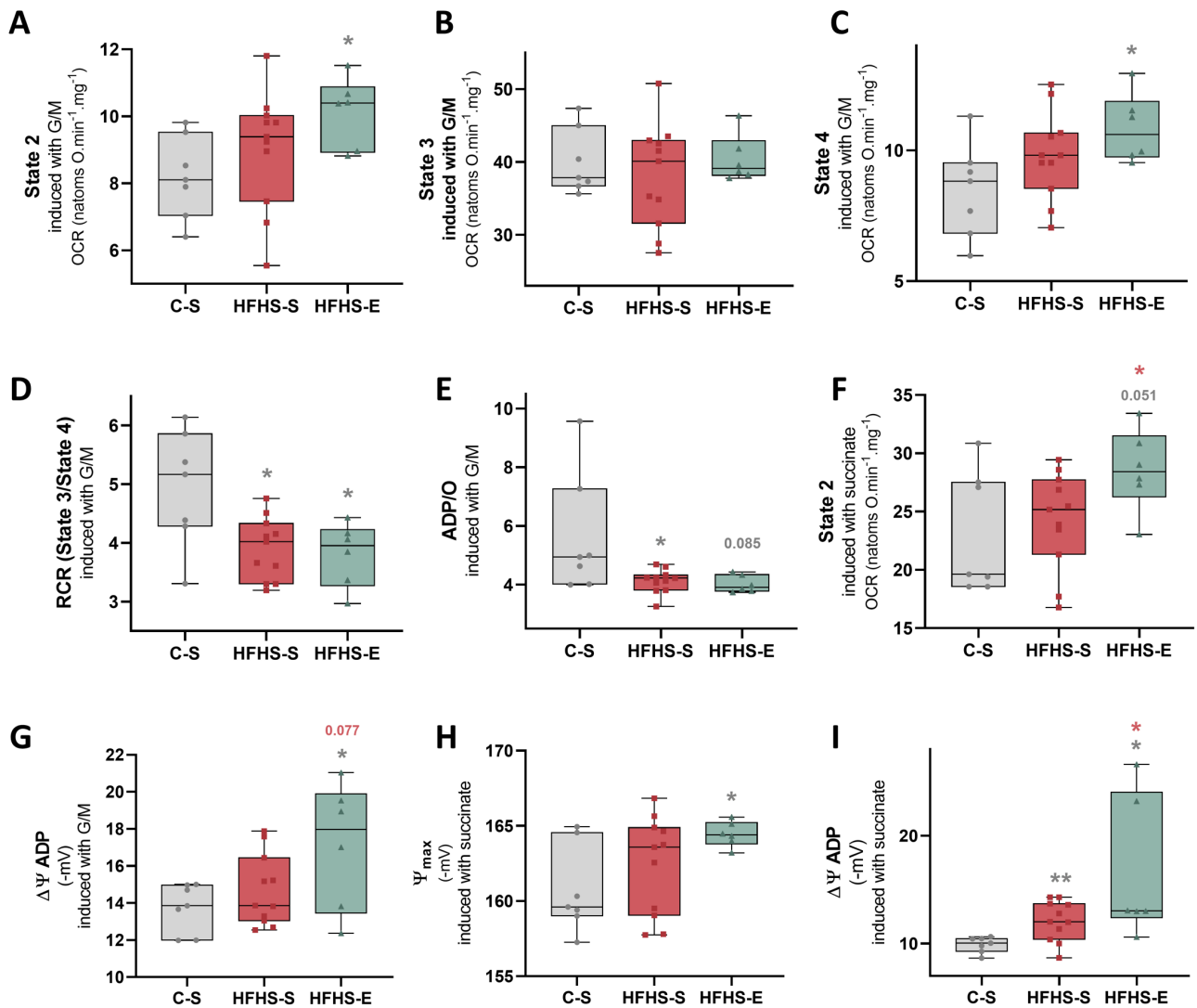


**Figure 5.** The impact of high-fat high-sugar diet and exercise on cardiac mitochondrial performance in the female hearts 8 weeks after exercise cessation. Cardiac mitochondrial oxygen consumption rates and using complex-I substrates glutamate/malate (G/M): (A) mitochondrial state 2 (basal respiration state), (B) mitochondrial state 3, (C) mitochondrial state 4 (D) RCR – respiratory control ratio (state 3/state 4 ratio), (E) amount of oxygen necessary to phosphorylate the added ADP (ADP/O) ratio. Cardiac mitochondrial oxygen consumption rates and using the complex-II substrate succinate: (F) mitochondrial state 2. Cardiac mitochondrial membrane potential using complex-I substrates glutamate/malate (G/M): (G) ADP-induced membrane depolarization ( $\Delta\Psi$  ADP). Cardiac mitochondrial membrane potential using the complex-II substrate succinate: (H) maximum mitochondrial membrane potential ( $\Psi_{max}$ ), (I)  $\Delta\Psi$  ADP. Comparison between the experimental groups was performed using unpaired t test or Mann-Whitney when one-way ANOVA  $p < 0.1$  and confirming normality with the Shapiro-Wilk normality test. \*  $p < 0.05$  HFHS-S vs C-S, or HFHS-E vs C-S, \*  $p < 0.05$  HFHS-E vs HFHS-S, \*\*  $p < 0.01$  HFHS-E vs C-S.



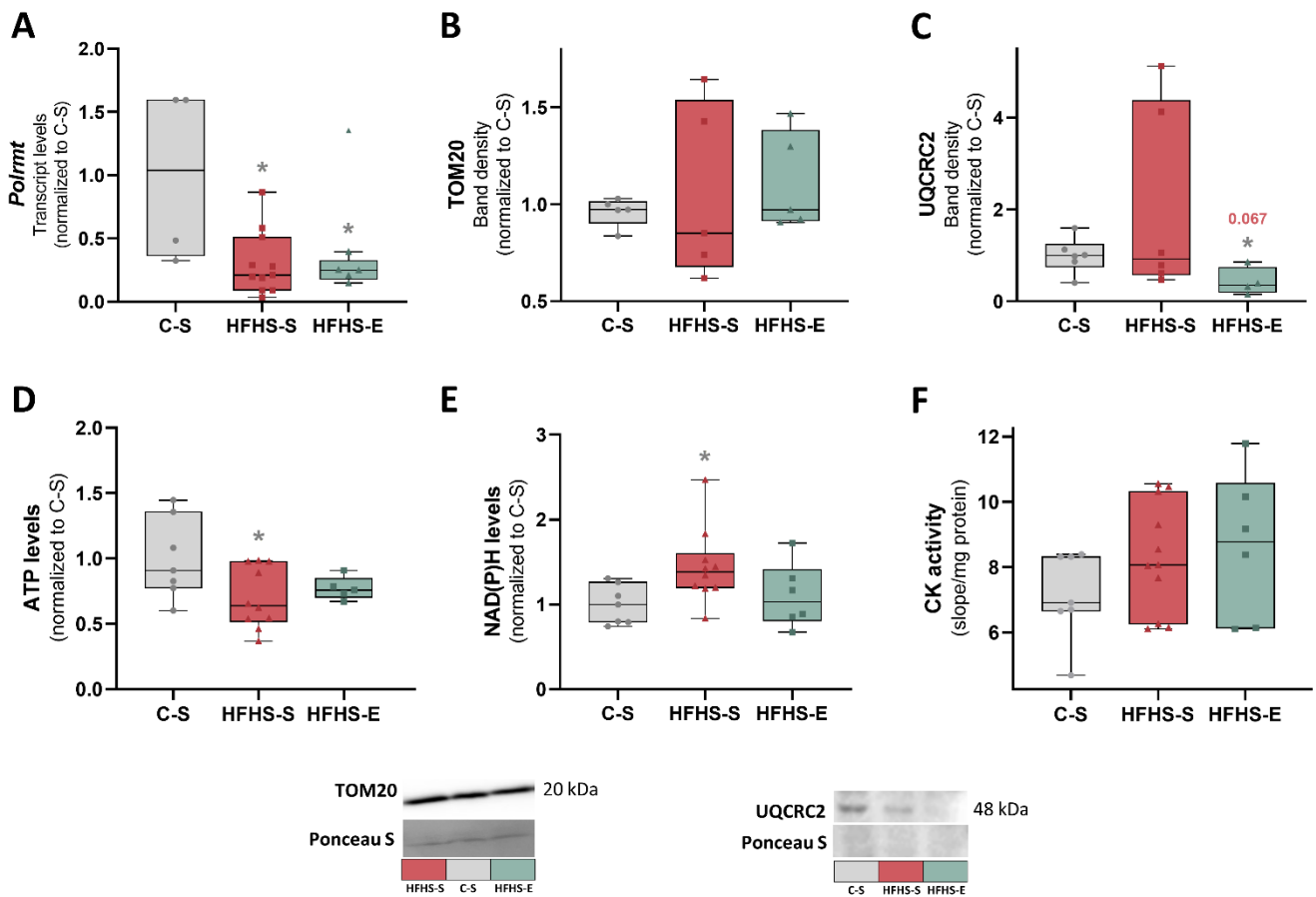


**Figure 6.** Effects of the HFHS diet and exercise cessation coupled to the HFHS diet on several mitochondrial biomarkers in female rats' hearts. (A) Transcript levels of *Polrmt* – mitochondrial RNA polymerase. Protein levels of (B) TOM20 and (C) UQCRC2, one of the subunits of complex II of the mitochondrial electron transport chain. Levels of (D) ATP and (E) NAD(P)H in the isolated cardiac mitochondrial fraction. (F) Enzymatic activity of creatine kinase (CK) in the cardiac tissue. Comparison between the experimental groups was performed using unpaired t test or Mann-Whitney when one-way ANOVA  $p < 0.1$  and confirming normality with the Shapiro-Wilk normality test. \*  $p < 0.05$  HFHS-S vs C-S, or HFHS-E vs C-S. Western blotting, PCR and ATP and NAD(P)H levels data were normalized to the average of C-S, considered = 1.

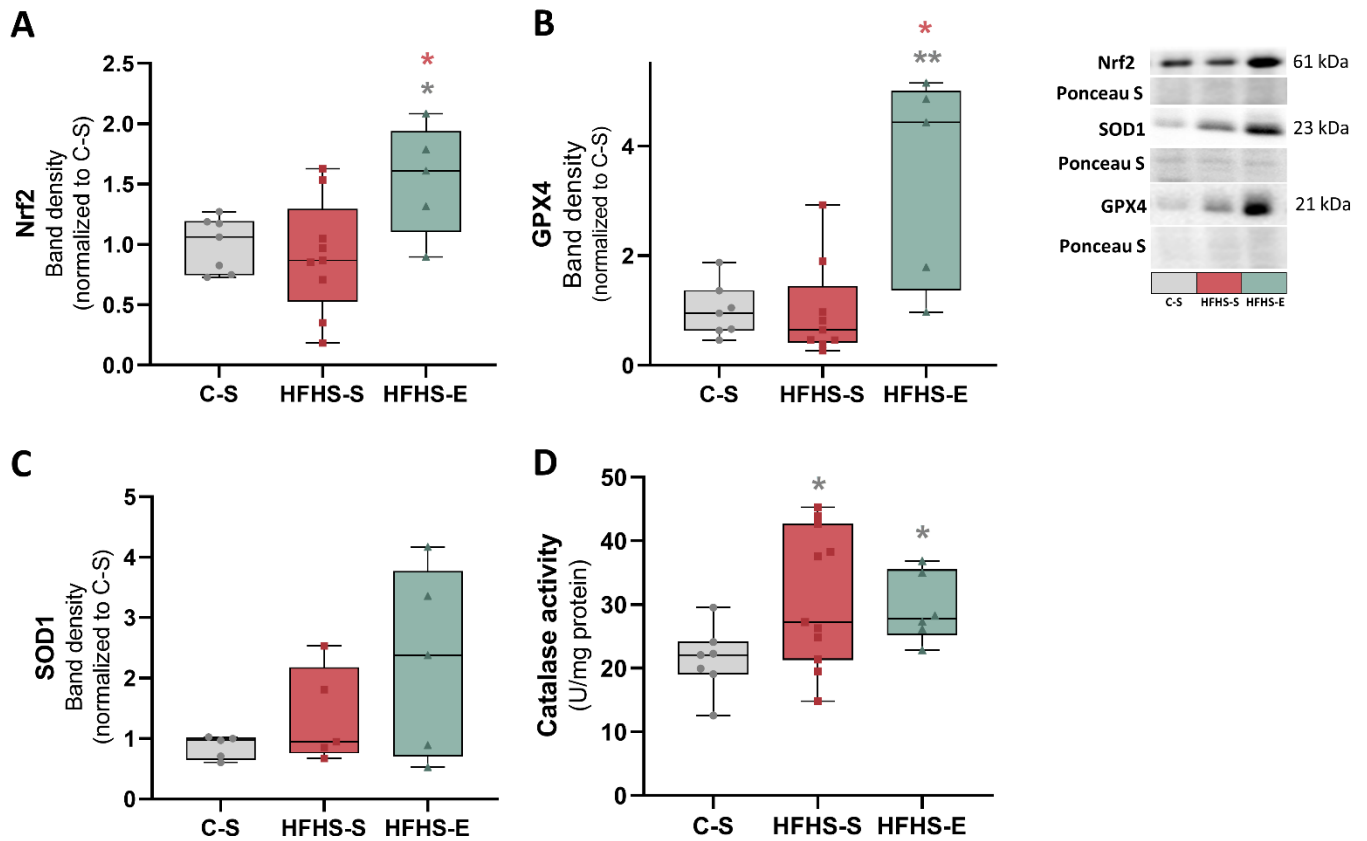


**Figure 7.** Cardiac redox balance in the response to the HFHS diet and physical exercise and subsequent cessation. Protein levels of (A) Nrf2 – Nuclear factor erythroid 2-related factor and directly related antioxidant proteins (B) GPX4 – glutathione peroxidase 4 and (C) SOD1 – superoxide dismutase 1. (D) Enzymatic activity of catalase. Comparison between the experimental groups was performed using unpaired t test or Mann-Whitney when one-way ANOVA  $p < 0.1$  and confirming normality with the Shapiro-Wilk normality test. \*  $p < 0.05$  HFHS-E vs C-S, \*  $p < 0.05$  HFHS-E vs HFHS-S, \*\*  $p < 0.01$  HFHS-E vs C-S. Western blotting data were normalized to the average of C-S, considered = 1.

Table S1

<b>Antibody</b>	<b>Manufacturer, reference</b>	<b>Dilution</b>
Cardiac troponin T	Cell Signaling, 5593	1:1000
IL-6	Santa Cruz, 28343	1:1000
TNF $\alpha$	Santa Cruz, 12744	1:1000
AKT	Cell Signaling, 2967	1:1000
p-AKT (Ser 473)	Cell Signaling, 2965	1:1000
p-AKT (Thr 308)	Cell Signaling, 4060	1:500
P70	Santa Cruz, 8418	1:1000
p-P70 (Thr 389)	Cell Signaling, 9205S	1:1000
GSK3 $\alpha$ , $\beta$	Santa Cruz, 7291	1:1000
p-GSK3 $\alpha$ , $\beta$ (Ser 21/9)	Cell Signaling, 9327	1:500
AMPK $\alpha$	Cell Signaling, 2603	1:1000
p-AMPK $\alpha$	Cell Signaling, 2531	1:1000
TOM20	Santa Cruz, 12744	1:1000
TFAM	Santa Cruz, 23588	1:1000
PGC1 $\alpha$	Calbiochem, ST1202	1:1000
FIS1	Santa Cruz, B76447	1:1000
DRP1	BD Bio Sciences, 611113	1:1000
OPA1	BD Bio Sciences, 612606	1:1000
MFN1	Santa Cruz, 50330	1:1000
MFN2	Sigma, 9927M3	1:1000
NRF2	Santa Cruz, 365949	1:1000
GPX4	Santa Cruz, 166570	1:500
SOD1	Santa Cruz, 515404	1:1000

Table S2

<b>Antibody</b>	<b>Manufacturer, reference</b>	<b>Dilution</b>
Anti-Goat	Santa Cruz, 2354	1:2000
Anti-Mouse	Cell Signaling, 7076S	1:2000
Anti-Rabbit	Cell Signaling, 7074S	1:2000

Table S3

<b>Gene</b>	<b>Reference</b>	<b>Forward primer sequence (5' - 3')</b>	<b>Reverse primer sequence (3' - 5')</b>
<i>Acox1</i>	NM_017340.2	GCAGACAGCCAGGTTCTTGATG	ACTCGGCAGGTCATTTCAGGTAT
<i>Hif1<math>\alpha</math></i>	NM_024359.1	CAAGCAGGAATTGGAACG	CTCATCCATTGACTGCCCCA
<i>Polrmt</i>	NM_001106766.1	GAGACAGGTACCTTCGATCTGG	GGTGGGTTTGTGTGTAGCCA
<i>Ppara</i>	NM_013196	AGACTAGCAACAATCCGCCTTT	TGGCAGCAGTGAAGAARCG
<i>Gapdh</i>	NM_017008.4	GTCATCCCAGAGCTGAACGG	ACTTGGCAGGTTTCTCCAGG
<i><math>\beta</math>-actin</i>	NM_031144.3	AGATCAAGATCATTGCTCCTCCT	ACGCAGCTCAGTAACAGTCC
<i>18S rRNA</i>	NR_046237.1	ACTCAACACGGGAAACCTC	ACCAGACAAATCGCTCCAC